Neutron Scattering Instruments of IBR-2 Reactor for Condensed Matter Research. Current State and Recent Results

D.P. Kozlenko

Frank Laboratory of Neutron Physics,
Joint Institute for Nuclear Research, 141980 Dubna, Russia

Modernized IBR-2 High Flux Pulsed Reactor (FLNP JINR)

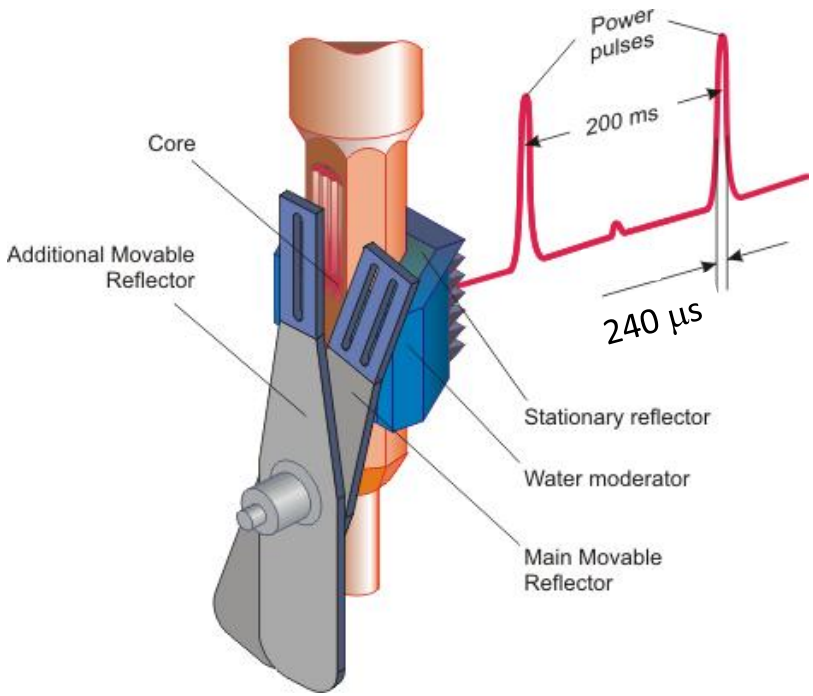

Information: http://flnp.jinr.ru/34/

Virtual excursion: http://uc2.jinr.ru/pano/lnf/

Operational since 1984

2007- 2010: modernization shutdown

2010 – 2011 Physical and power start-up completed

2012 – Regular operation renewed

Technical parameters of IBR-2M

Parameter	IBR-2	IBR-2M
• Thermal neutron flux in pulse, n/cm^2/c	5·10^{15}	5·10^{15}
• Average power, MW	2	2
• Power in pulse, MW	1850	1850
• Fuel	PuO_2	PuO_2
• No. fuel elements	78	69
• Max. fuel burn up,%	6,5	9
• Repetition rate, Hz	5	5
• Pulse width, μs	215	240
• RPM of movable reflector blades		
– main	1500	600
– auxiliary	300	300
– No. of satellite pulses	4	1

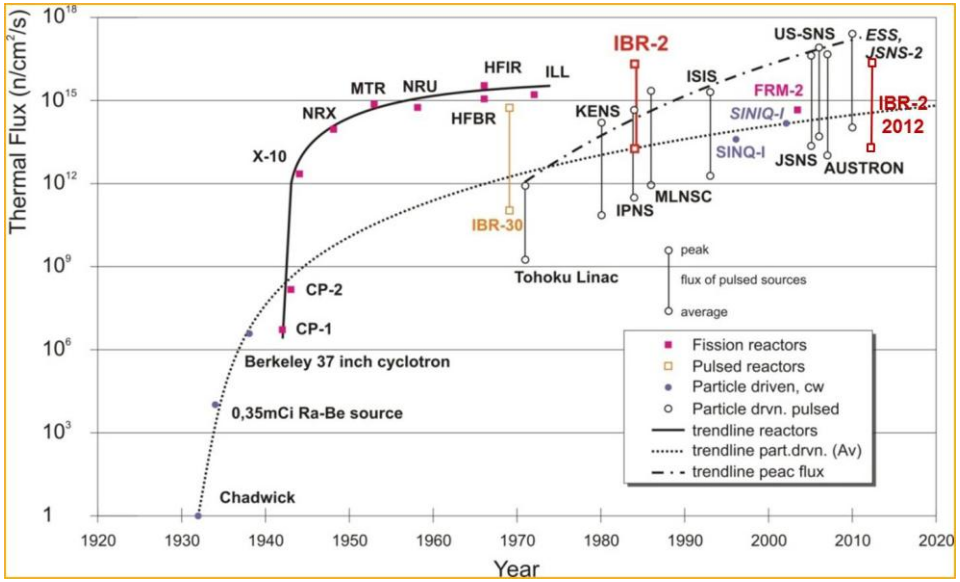

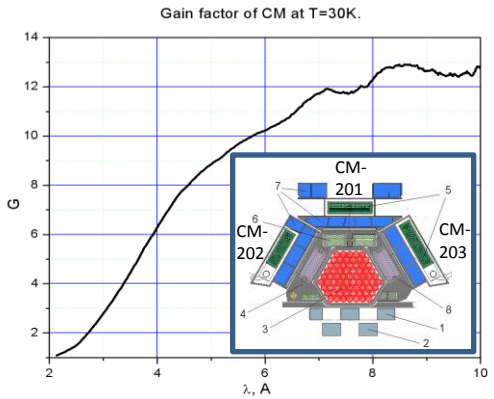

Pelletized cryogenic moderator of IBR-2

IBR-2M Spectrometers Complex

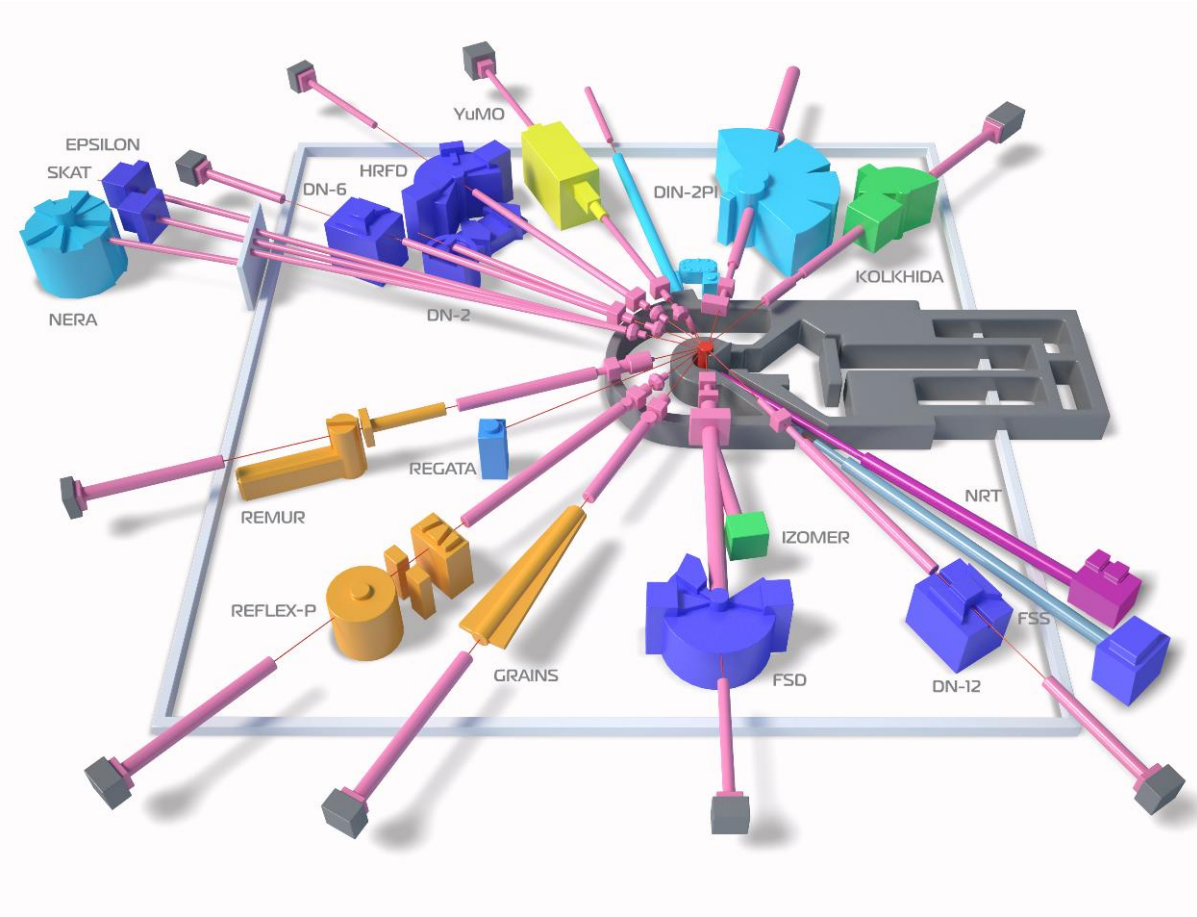

Diffractometers:

HRFD, DN-12, FSD, SKAT/Epsilon

Reflectometers:

REMUR, REFLEX

Small Angle Scattering Spectrometer: YuMO

Inelastic Neutron Scattering Spectrometers:

NERA-PR, DIN-2PI

New Instruments:

DN-6. GRAINS, NRT

Reconstruction:

DN-2 – RTD,

REFLEX - SESANS

2011:
11 instruments in operation

→

2014:
14 instruments in operation

The priority directions of fundamental research :

- Nanoscale physics

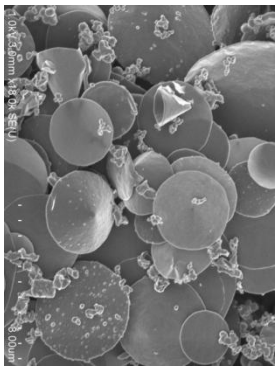

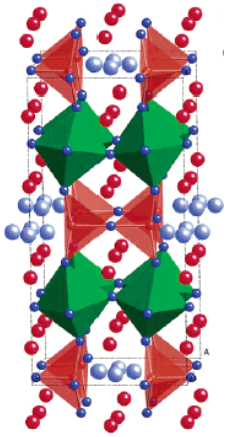

- Physics and Chemistry of Functional Materials

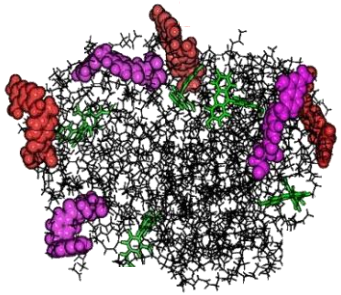

- Physics and Chemistry of Complex Liquids and Polymers

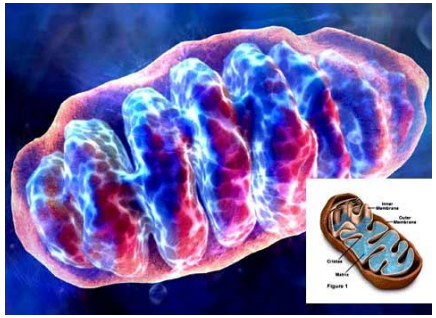

- Physics of Soft Condensed Matter

The priority directions of applied research:

- **Structural characterization of functional materials used in different (nano)technologies**

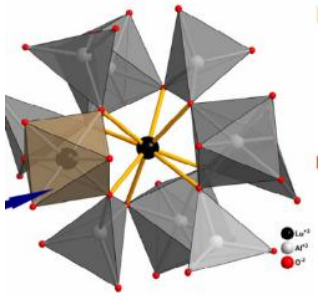

- **Non-destructive control of residual stresses and internal organization of bulk materials and products**

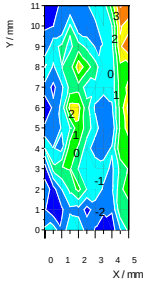

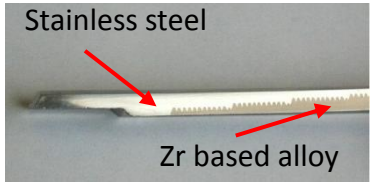

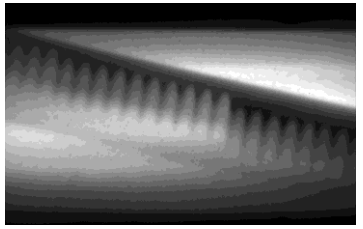

- **Texture analysis of geomaterials and constructional materials**

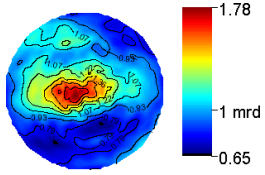

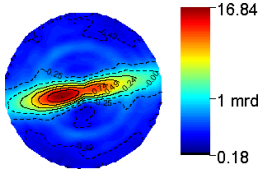

User Programme at IBR-2 instruments:

Two calls of proposals per year with deadlines 15 April and 15 October

Applications are collected via web-site http://ibr-2.jinr.ru

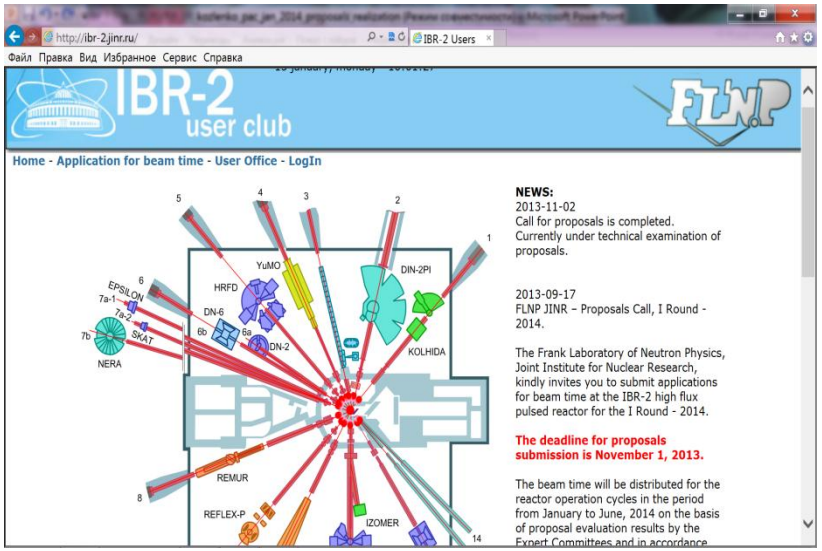

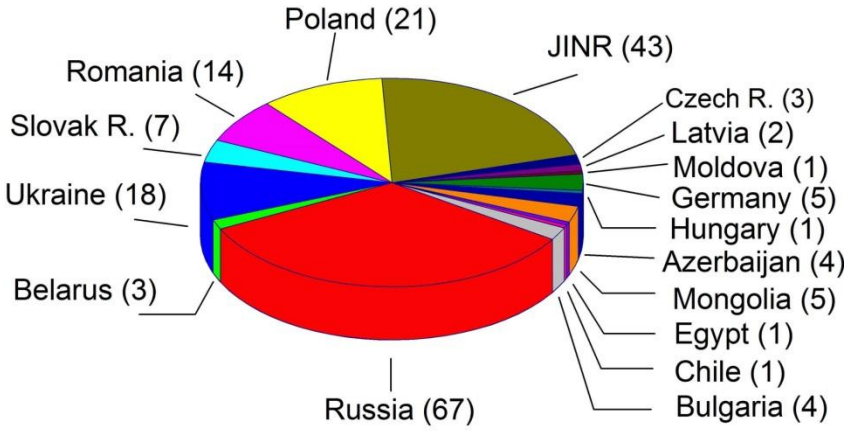

200 applications from 16 countries were received in 2013

HRFD

Precise structural studies of crystalline materials using reverse TOF method, $\Delta d/d \sim 0.001$

DN-2

Reconstruction to real time diffractometer (RTD)

Real time studies

Diffraction (fundamental research)

DN-12

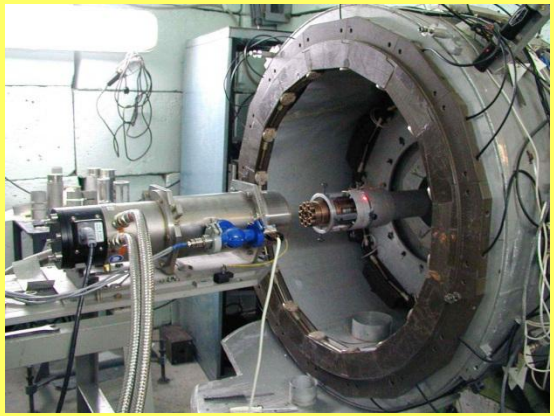

Studies of structure and dynamics of condensed matter under extreme conditions (P ~ 7 GPa)

DN-6

In operation since 2012

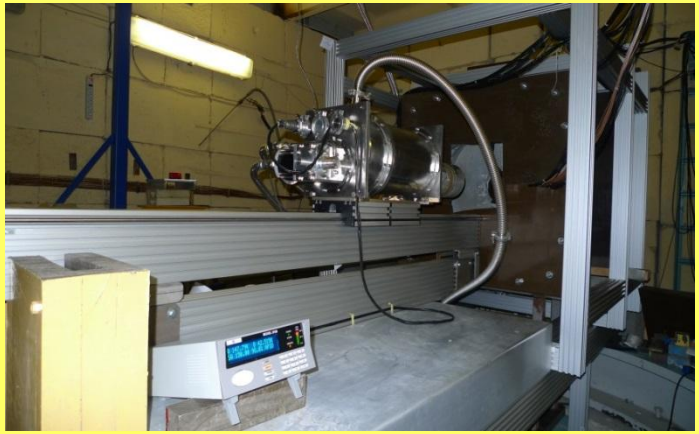

Structural studies at ultrahigh pressures (up to 30-50 GPa)

High Resolution Fourier Diffractometer

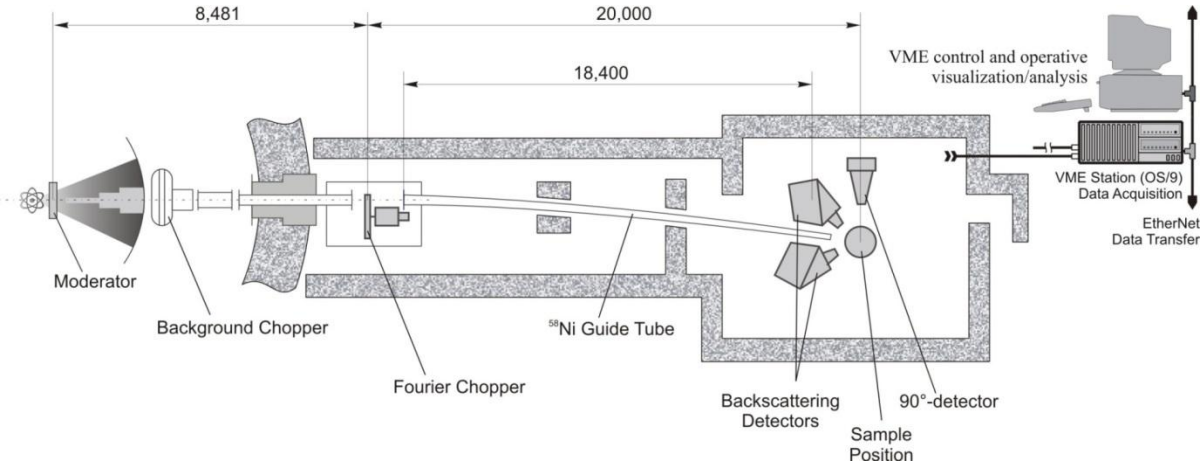

Neutron flux at sample position: 10^7 n/cm^2/s

Resolution at d = 2 Å, 2θ =152^0: Δd/d = 0.0008

D-spacing range in high resolution mode: 0.7- 4 Å

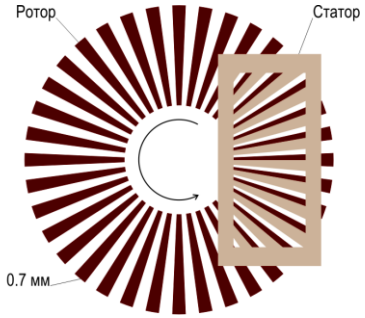

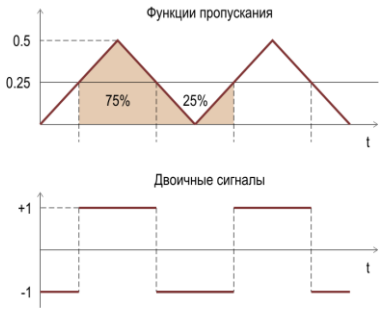

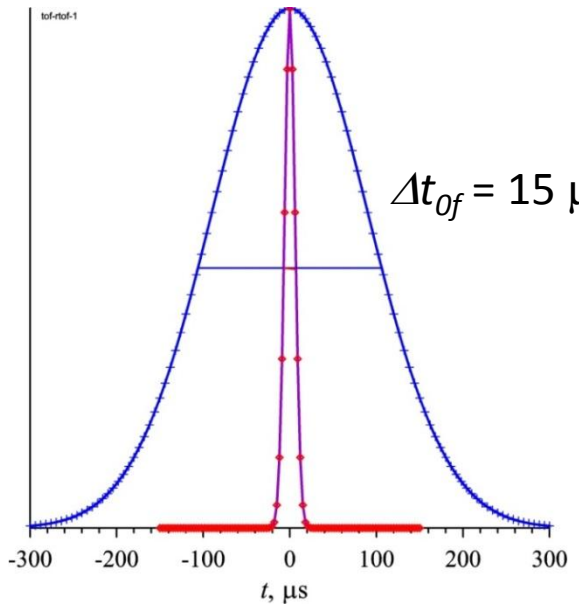

Δt_{0f} = 15 μs

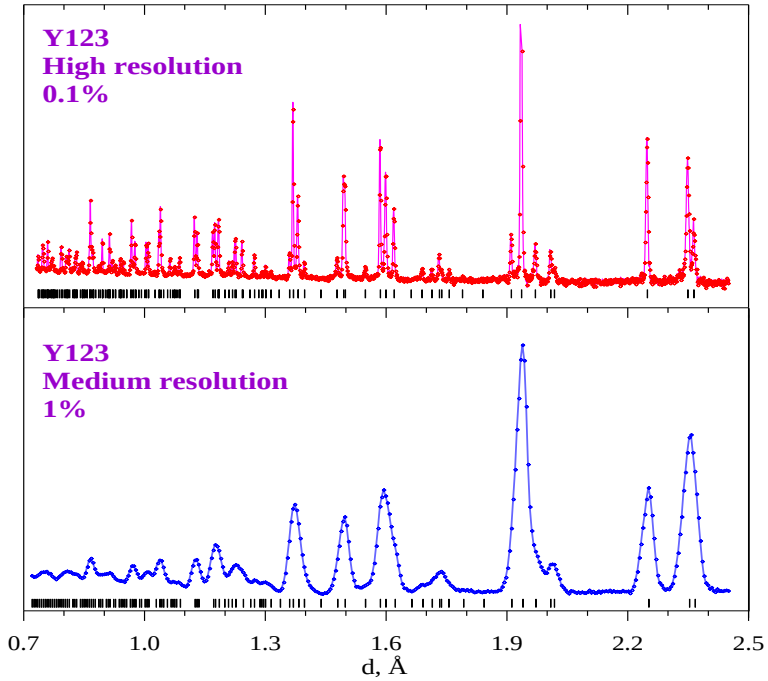

$$I(\omega, t) \sim \int_0^t \sigma(\tau)\cdot R[(\tau - t), \omega]\, d\tau$$

DN-12 Spectrometer for Studies of Microsamples

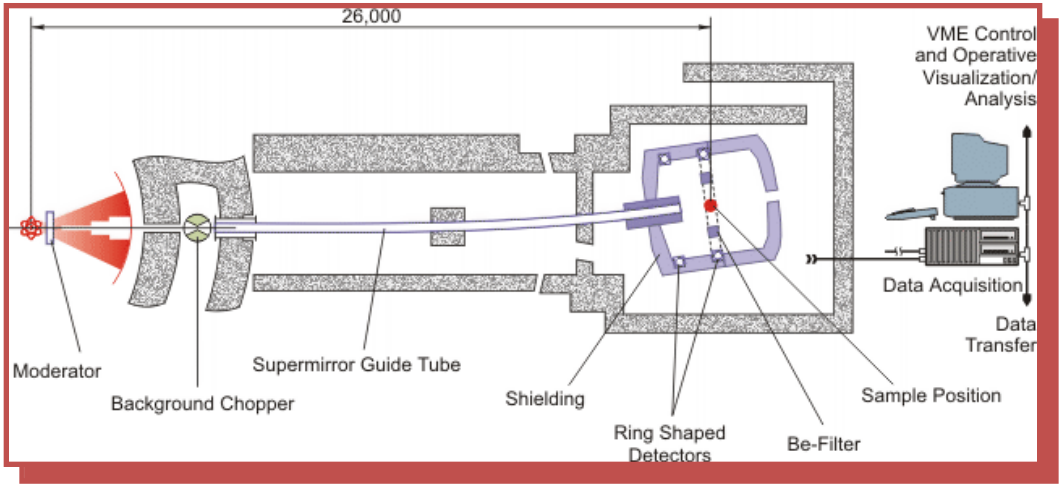

Neutron flux at sample position: $2 \cdot 10^6$ n/cm^2/s

Resolution at d = 2 Å, $2\theta = 90^0$: $\Delta d/d = 0.02$

D-spacing range: 0.8 - 13 Å

Pressure range: 0 – 7 GPa

Temperature range: 10 – 300 K

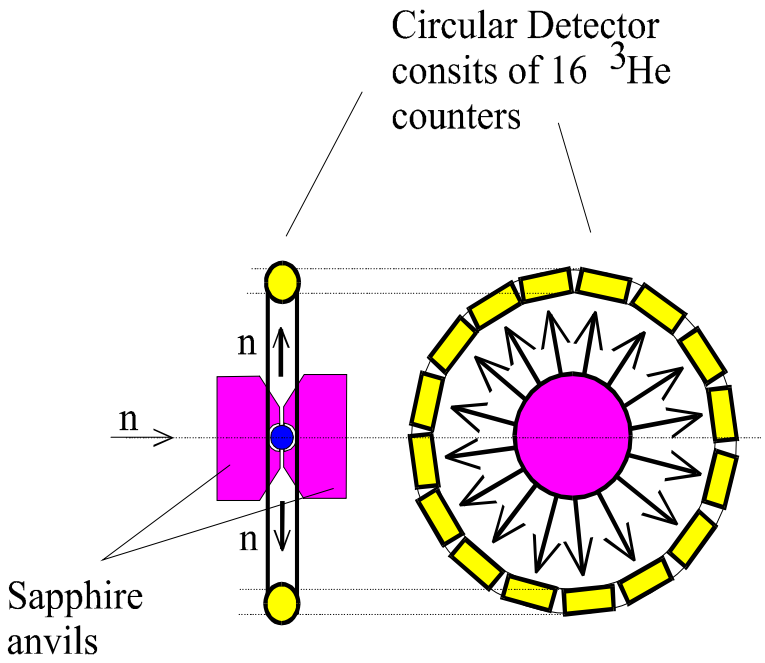

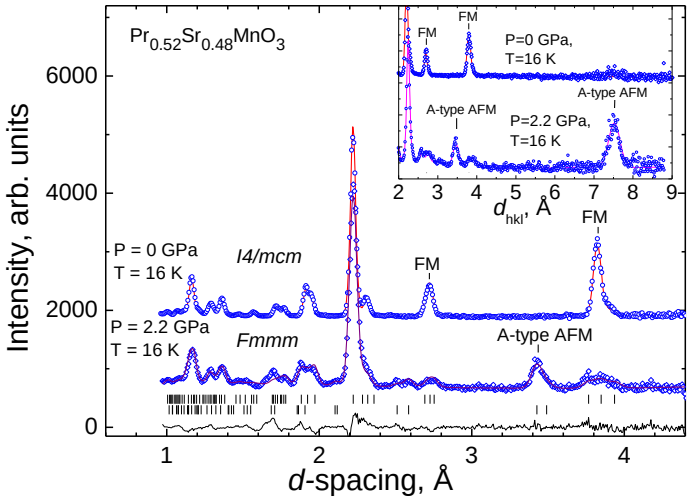

Pressure cell with sapphire anvils

Diffractometer DN-6 for studies of microsamples under extreme conditions

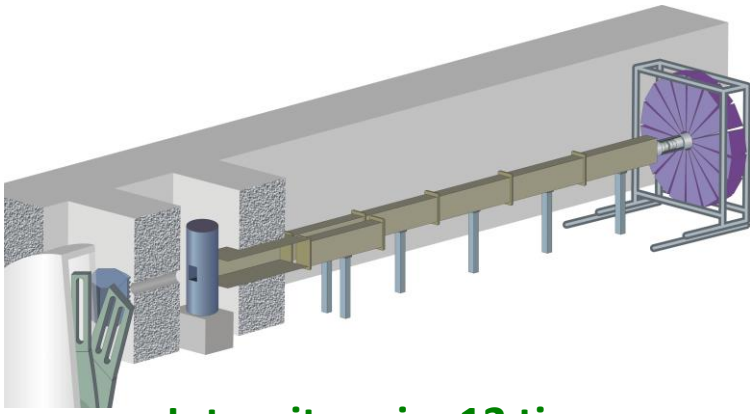

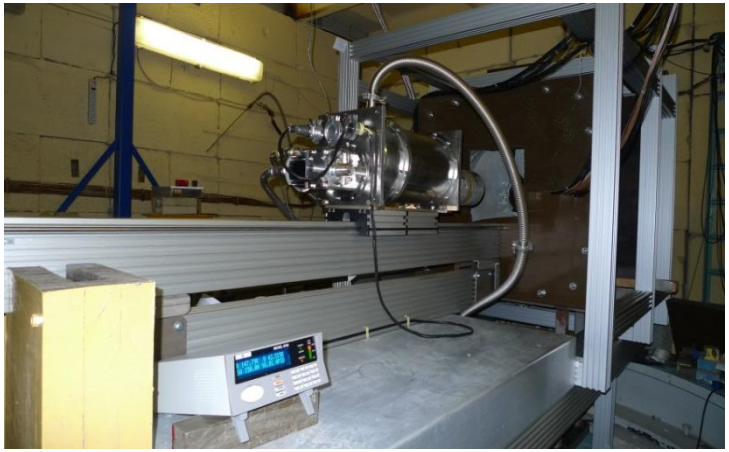

DN-6 diffractometer

DAC

- Intensity gain: 12 times (compared to DN-12)
- Pressure range: 30-50 GPa
- Temperature range: 4– 300 K

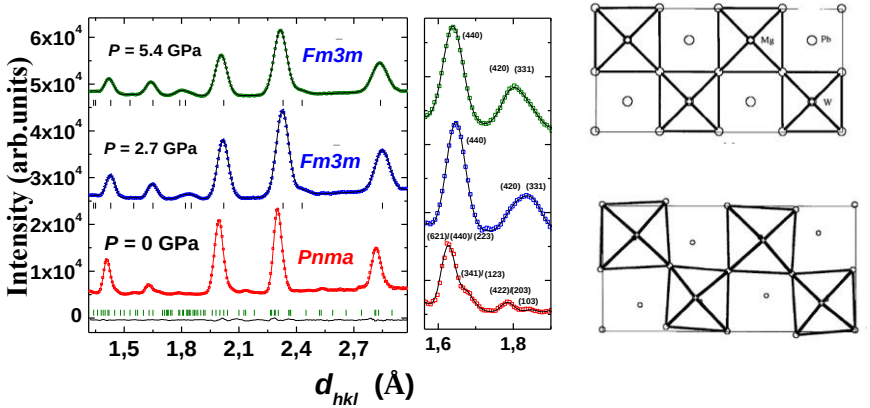

Neutron diffraction studies of structural phase transition in $PbMg_{1/2}W_{1/2}O_3$ perovskite under pressure (proposal from Institute of Physics, Azerbaijan), published in Phys. Solid State (2014)

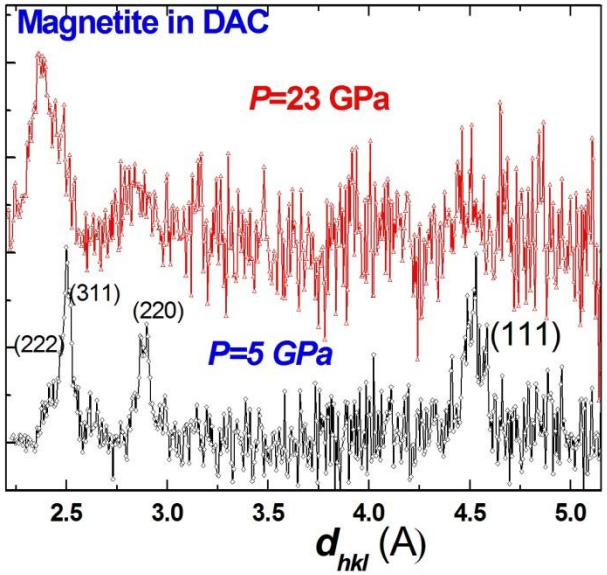

Neutron diffraction patterns of Fe_3O_4 sample measured in DAC at P = 5.5 and 23 GPa

Diffraction (applied research)

FSD

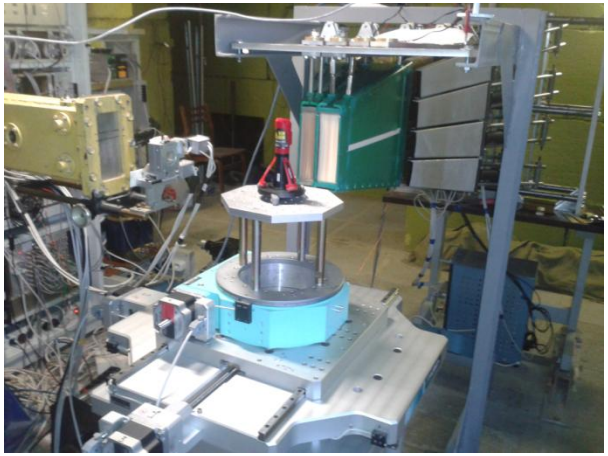

Determination of residual stresses in construction materials, industrial materials and factory-made goods using RTOF method

$\Delta d/d \sim 0.002$

SKAT

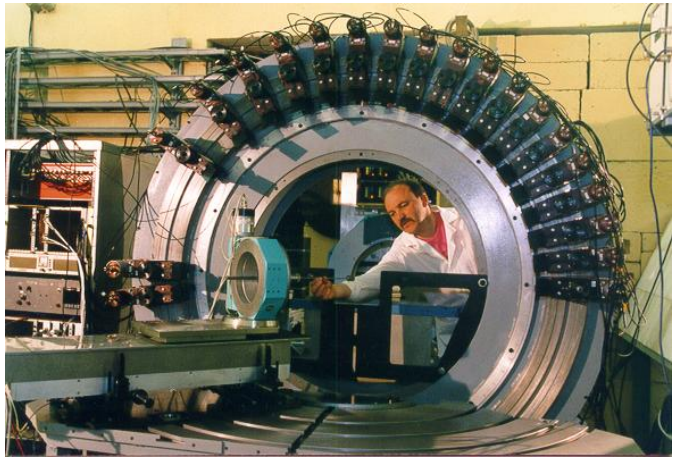

Texture analysis of geological materials (rocks, minerals) and constructional materials

EPSILON-MDS

Residual stress analysis in geological materials (rocks, minerals)

High resolution due to long flight path L ~ 105 m

$\Delta d/d \sim 0.003\text{-}0.004$

Major modernization focused on replacement of neutron guides was finished by 2012

YuMO - SANS

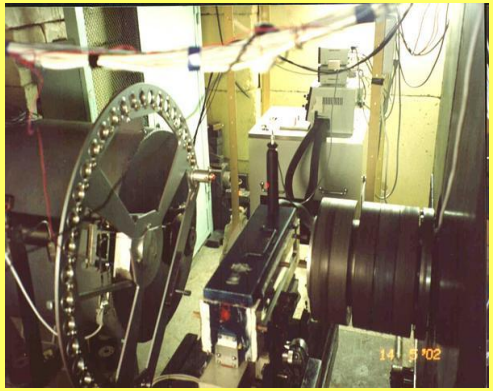

A study of structural characteristics of nanostructured materials, biological objects, polymers

REMUR

Reflectometer with polarized neutrons

A study of magnetization profile, magnetic and structural properties of layered nanostructures

Small Angle Neutron Scattering and Reflectometry

REFLEX

Reflectometer with polarized neutrons

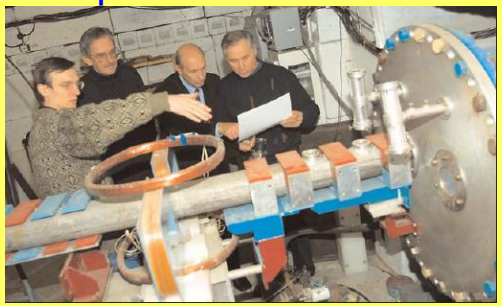

A study of structural properties of thin films and layered nanostructures

Reconstruction into Spin Echo Small Angle Neutron Scattering Spectrometer

GRAINS

Multifunctional reflectometer

A study of structural properties of liquid and soft matter interfaces

YuMO Small Angle Scattering Spectrometer

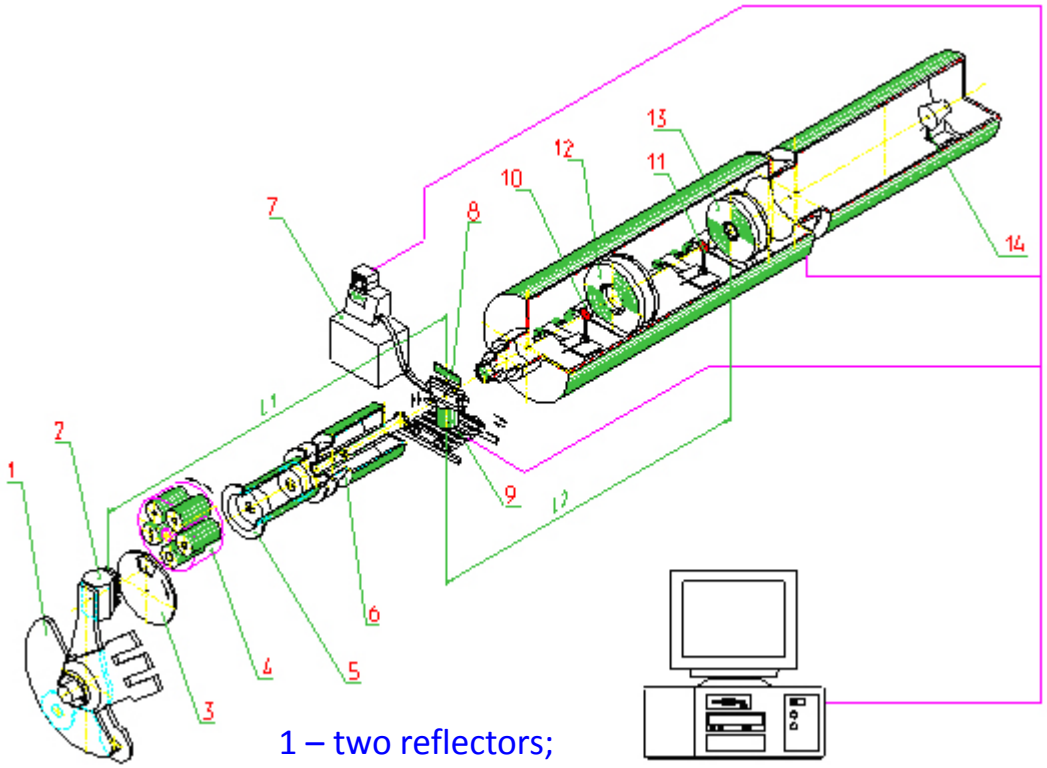

L_1 =17.8 m, L_2 =13.2 m

Neutron flux at sample position: $4 \cdot 10^7$ n/cm^2/s

Q-range: $7 \cdot 10^{-3}$ - 0.5 Å^{-1}

Q-resolution: 5-20 %

Typical measurement time: 1 h

1 – two reflectors;
2 – zone of reactor with moderator;
3 – chopper;
4 – first collimator;
5 – vacuum tube;
6 – second collimator;
7 – thermostate;
8 – samples table;
9 – goniometer;
10-11 – Vn-standard;
12 – ring-wire detector;
13 – position-sensitve edetector "Volga";
14 – direct beam detector.

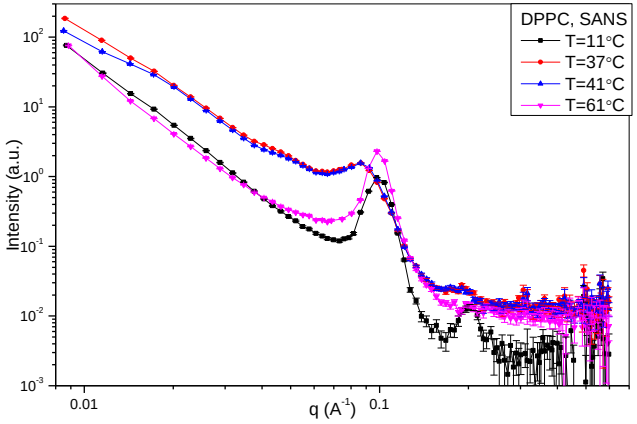

REMUR - Reflectometer with polarized neutrons

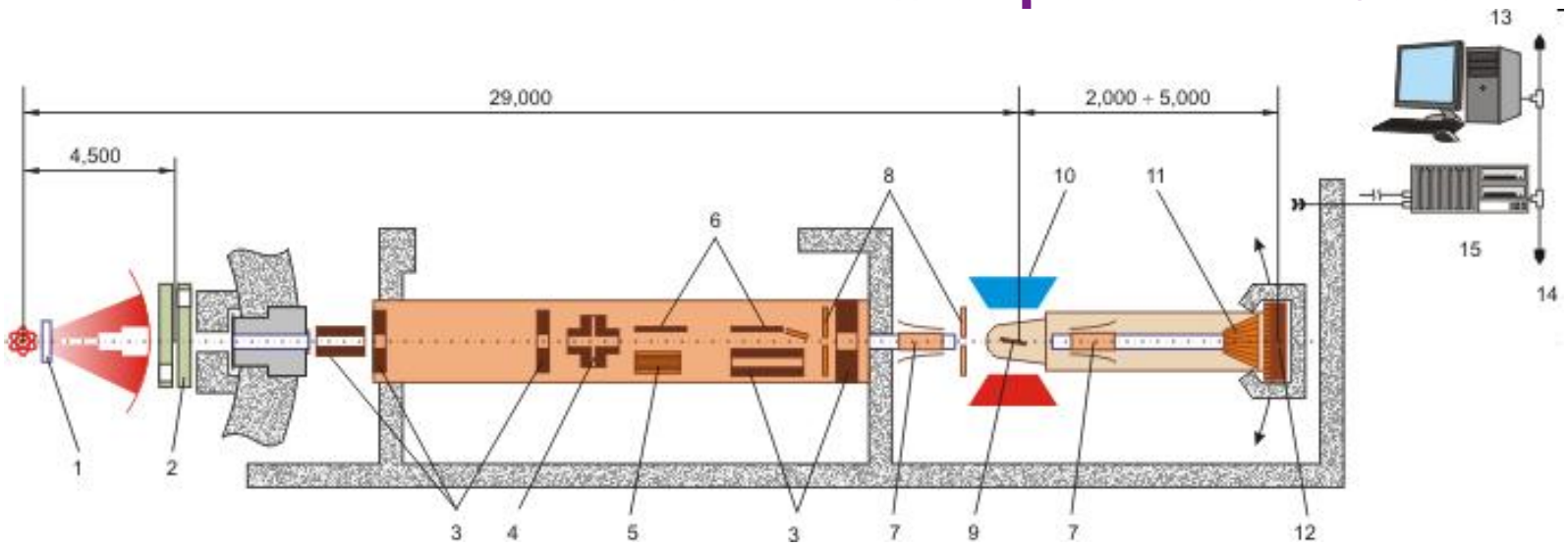

1 - Moderator
2 - Double Disk Background Chopper
3 - Collimators
4 - Cross-type Collimator
5 - Small-Angle Scattering Mode Polarizer
6 - Adjustable Platforms
7 - Spin-Flipper
8 - Variable Diaphragms
9 - Sample Position
10 - Electromagnet
11 - Fan Polarization Analyzer
12 - Position-Sensitive Detector
13 - Control and operative visualization/analysis
14 - Data Acquisition
15 - Data Transfer

Neutron flux at sample position: $3 \cdot 10^4$ n/cm^2/s

λ-range: 0.9 - 10 Å^{-1}

2θ range: 1-100 mrad

$\Delta\lambda/\lambda$: 2 %

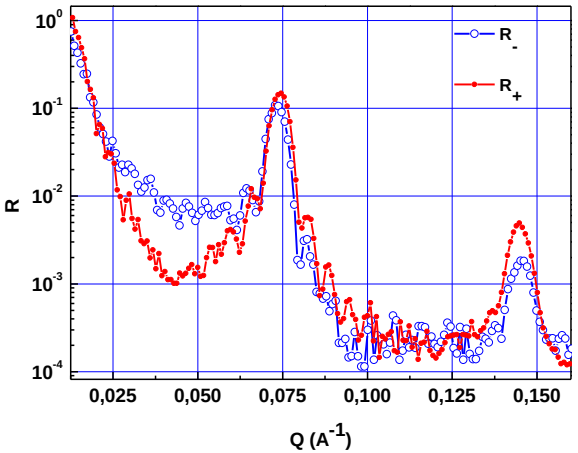

Reflection coefficients from

12×[Fe(35Å)Cr(4.4 Å)/Gd(50 Å)]

Multifunctional reflectometer GRAINS

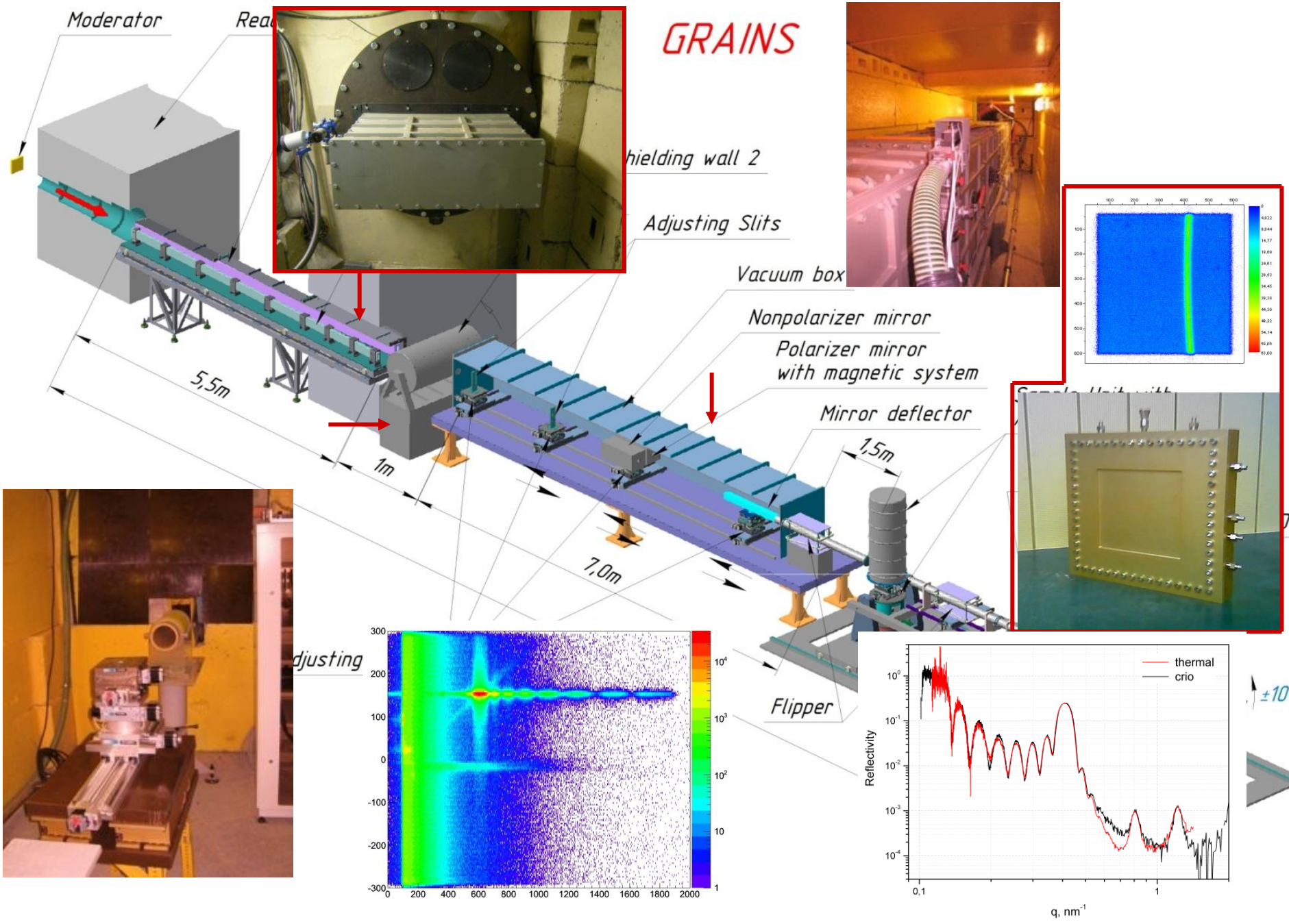

Inelastic Neutron Scattering

NERA-PR

Vibrational spectra of molecular crystals

DIN-2PI

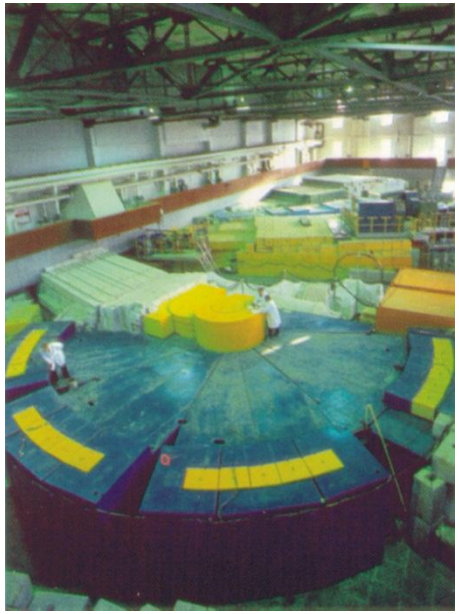

Lattice dynamics, atomic dynamics of liquids and amorphous materials

DN-12

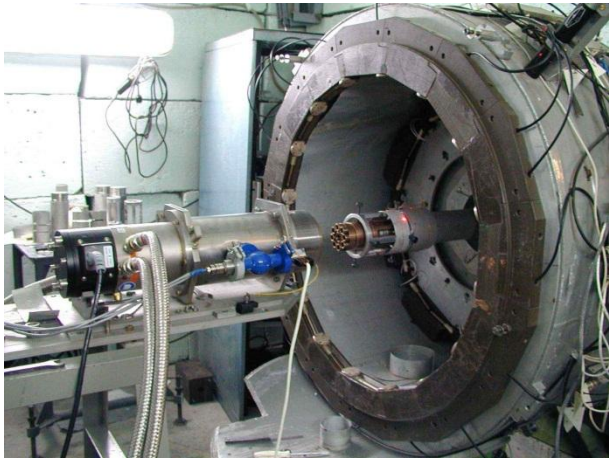

Vibrational spectra of hydrogen-containing materials under pressure up to 5-10 GPa

NERA-PR – Inelastic Neutron Scattering Spectrometer in Inverted Geometry

Neutron flux at sample position:
$4 \cdot 10^6$ n/cm²/s

Energy transfer range:
0-500 meV

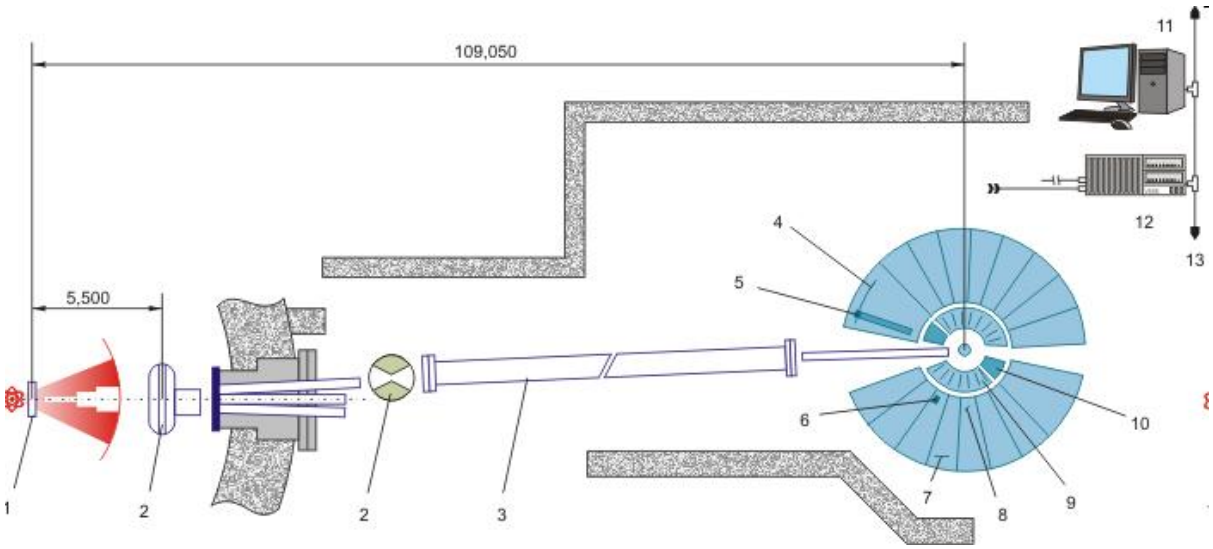

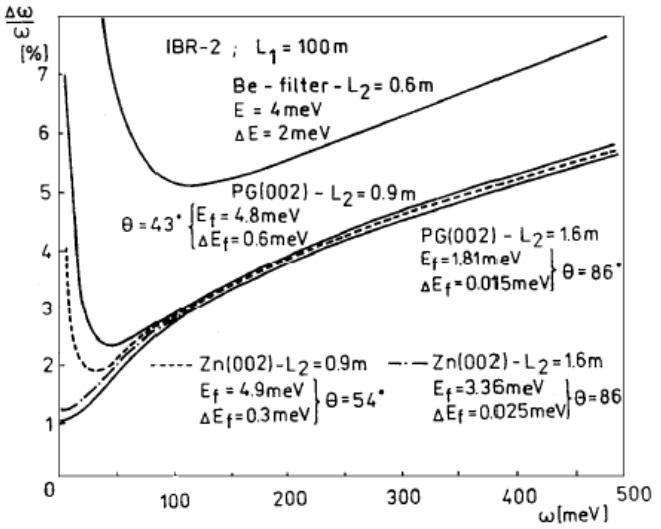

1 - Moderator
2 - Background Choppers
3 - Ni Guide Tube
4 - Detector for High Intensity Diffraction
5 - Detector for High Resolution Diffraction
6 - He3 Detectors (INS and QNS)
7 - Single Crystal QNS Analyzer
8 - Pyrolytic Graphite INS Analyzer
9 - Be-Filters
10 - Collimators
11 - VME control and operative visualization/analysis
12 - VME Station (OS/9)Data Acquisition
13 - EtherNet Data Transfer

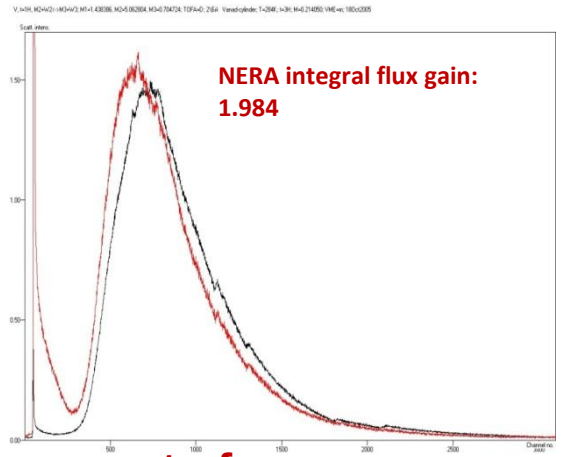

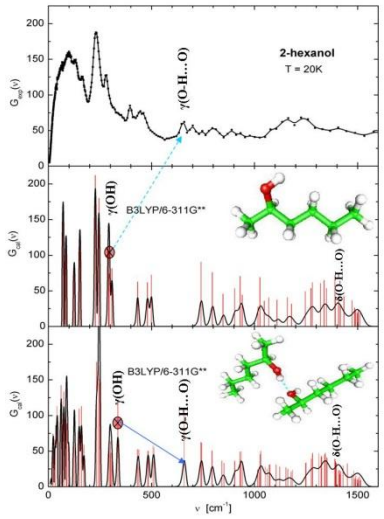

Major modernization focused on replacement of neutron guide was finished by 2012

DIN-2PI – Inelastic Neutron Scattering Spectrometer in Direct Geometry

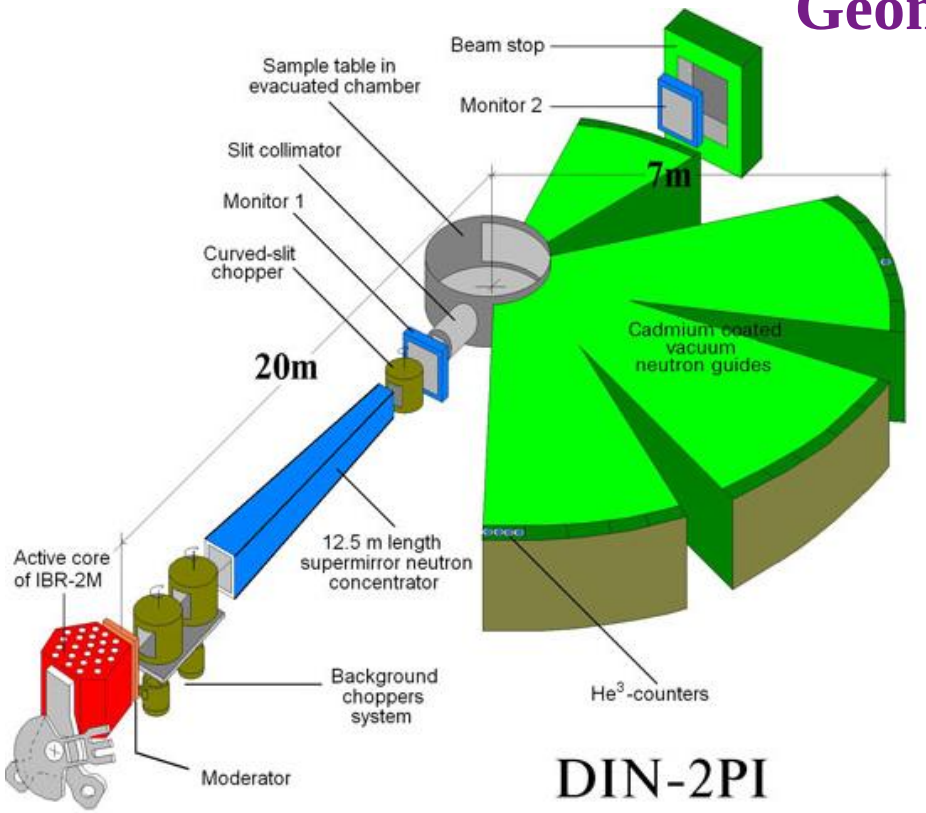

Neutron flux at sample position: $4 \cdot 10^6$ n/cm^2/s

2θ range: 5-135^0

Incident neutron energy range: 1-300 meV

Energy resolution: $\Delta E/E$ = 4-10 %

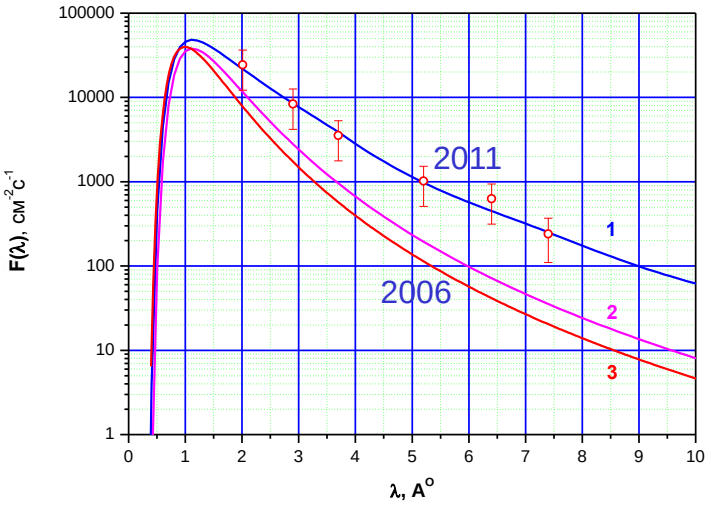

Installation of neutron concentrator gives an order of magnitude increase of neutron flux at sample position

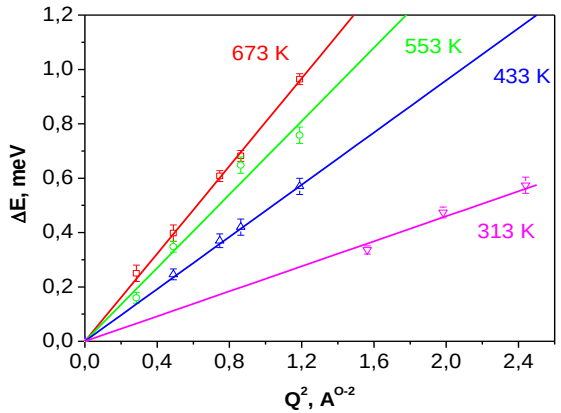

FWHM of incoherent QENS peak in liquid Ga

Instrument for neutron imaging at 14 beamline of IBR-2M: Current State

Biological schielding

Vacuumed collimator

CCD-based detector and sample position

CCD Camera Videoscan

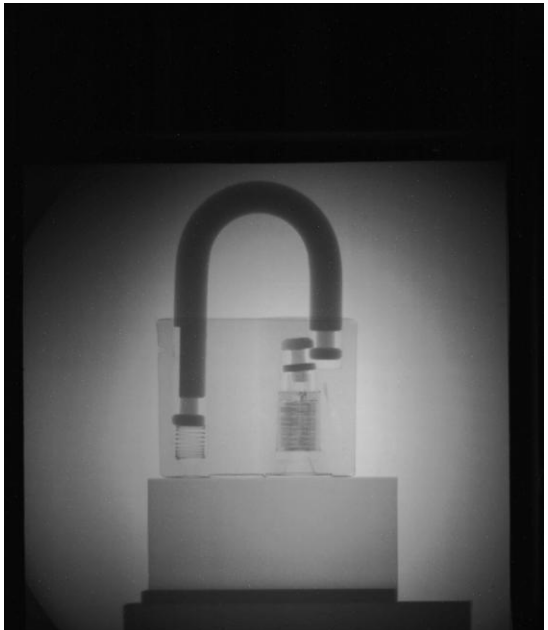

IBR-2M Spectrometers Complex:

Further Developments

RTD diffractometer for real-time studies

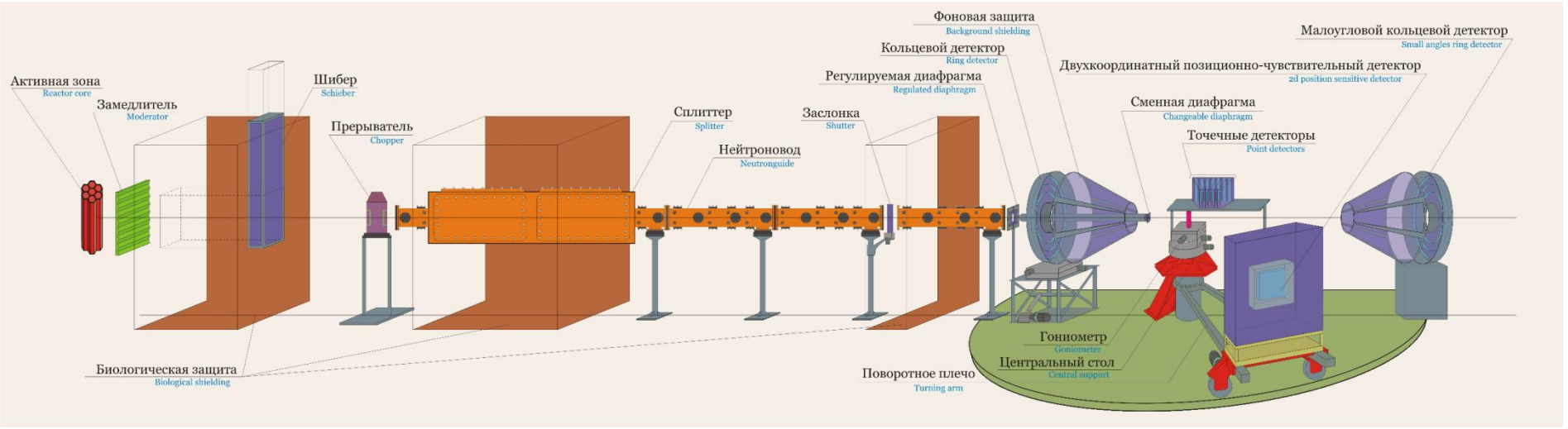

Ring-shaped helium backscattering detector on the RTD diffractometer

Adjustable neutron beam diaphragm for the RTD diffractometer 20x105mm

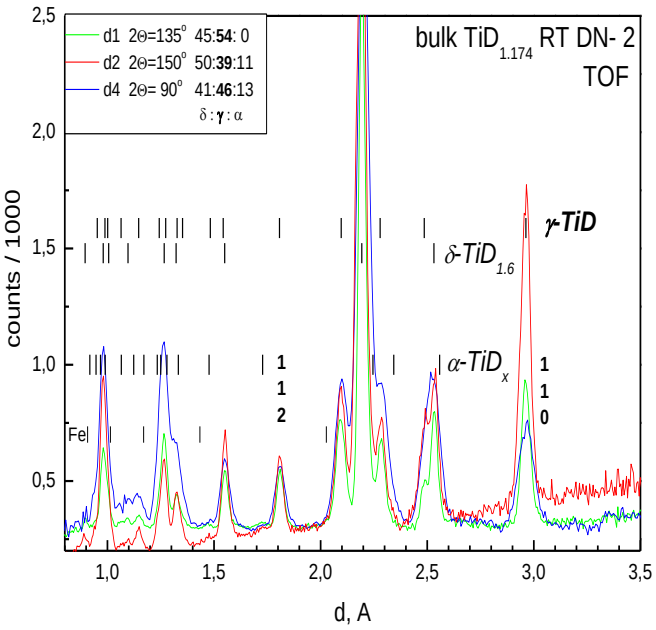

Fedotov V.K., Sholin I.A., Beskrovniy A.I., Sheverev S.G.

FSS diffractometer, beamline 13

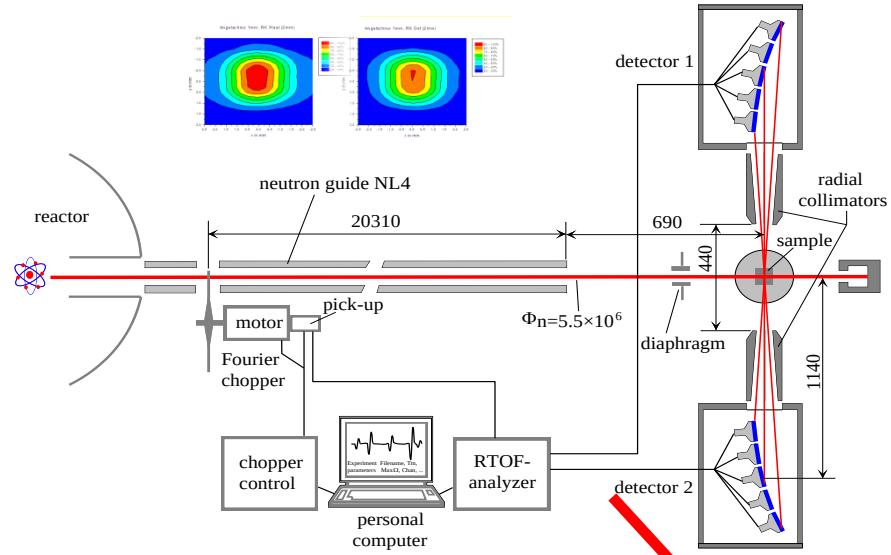

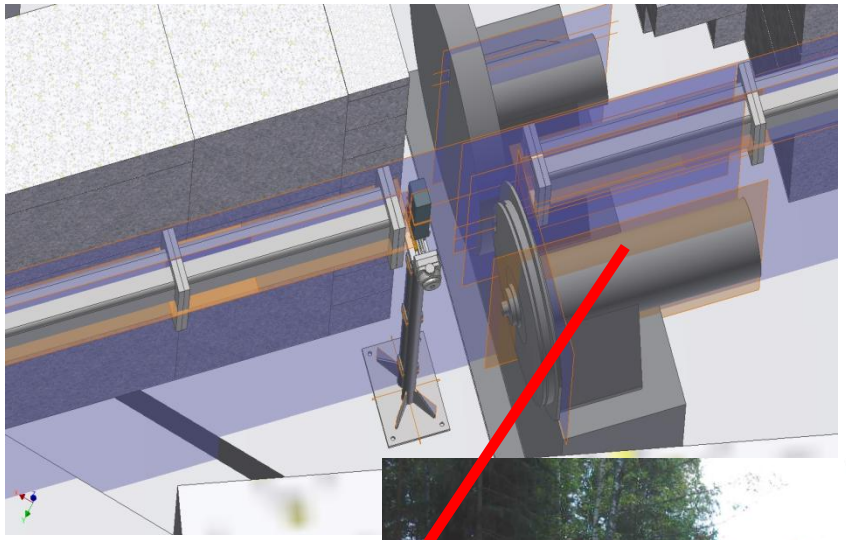

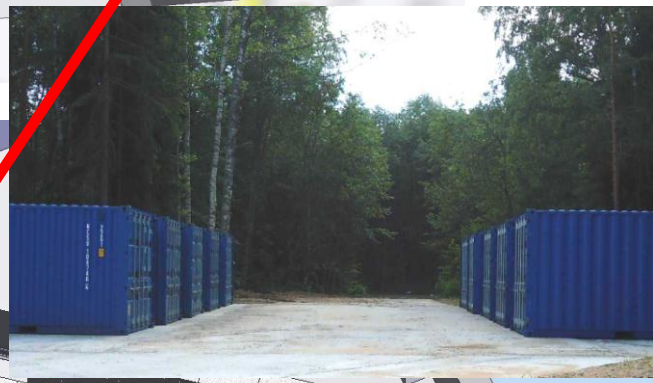

Stress rig

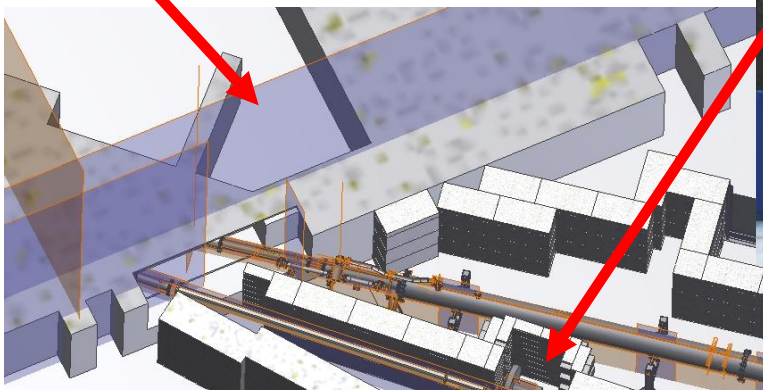

+air heaters

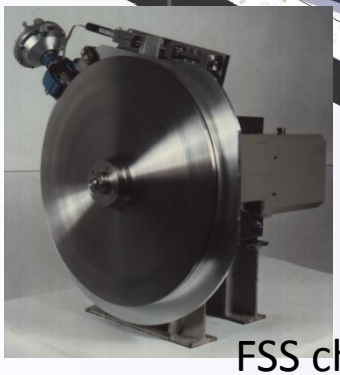

FSS chopper

Spin Echo Small Angle Neutron Scattering Spectrometer in construction on the Basis of REFLEX Reflectometer

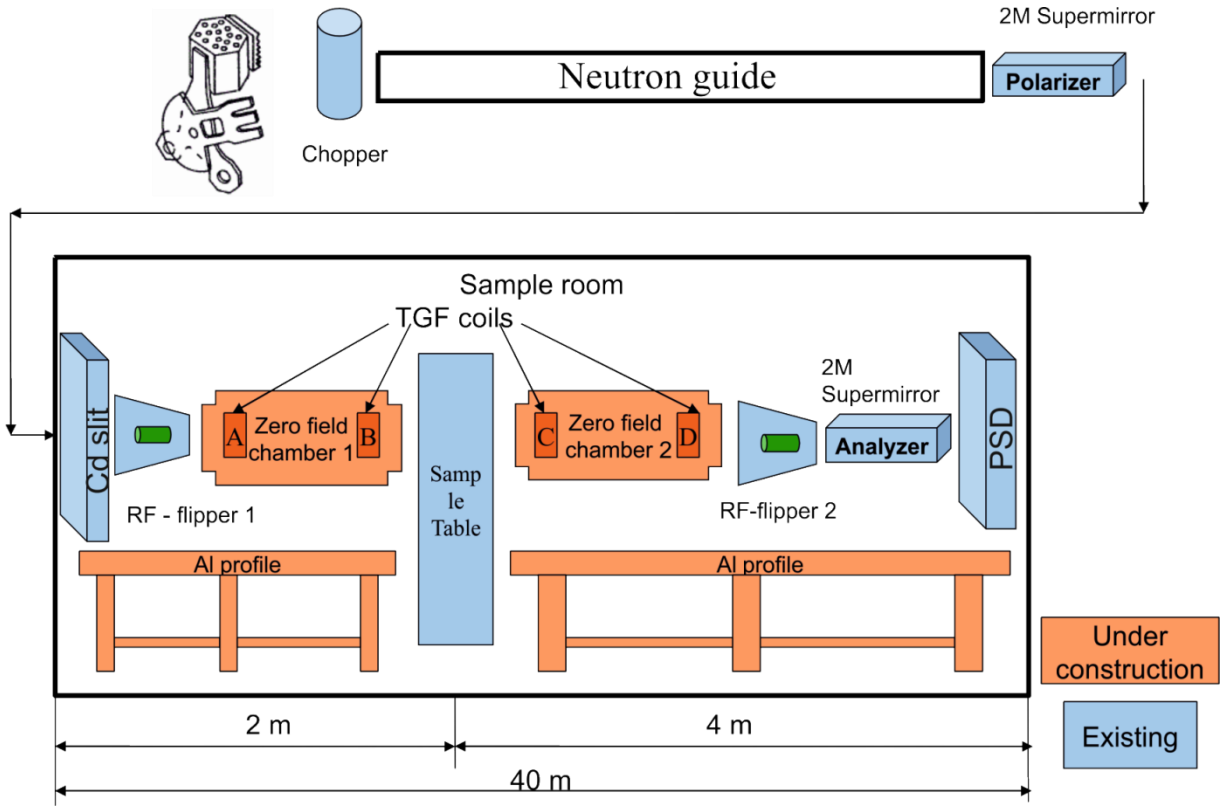

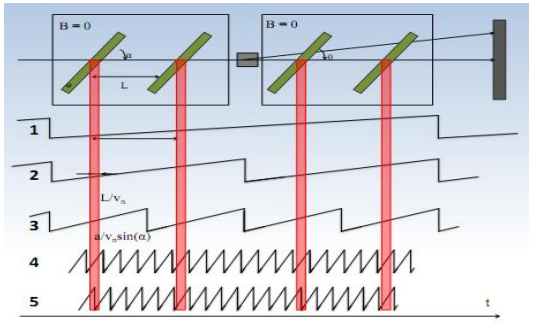

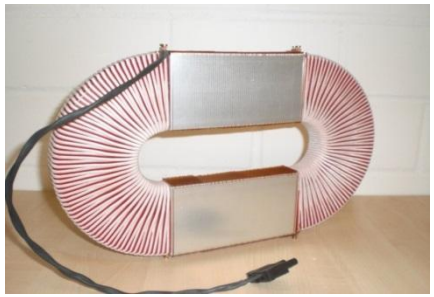

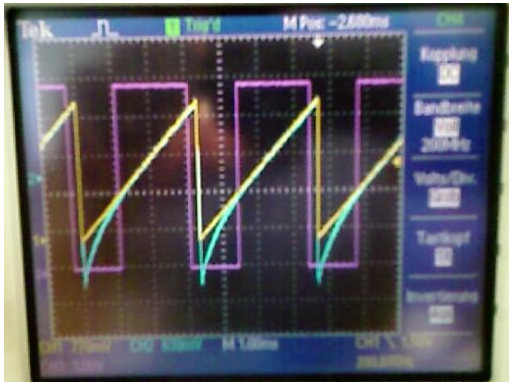

Time gradient magnetic fields

Overview of recent scientific results

Real-time studies of structural changes in Li-based accumulators during charging and discharging processes with high resolution

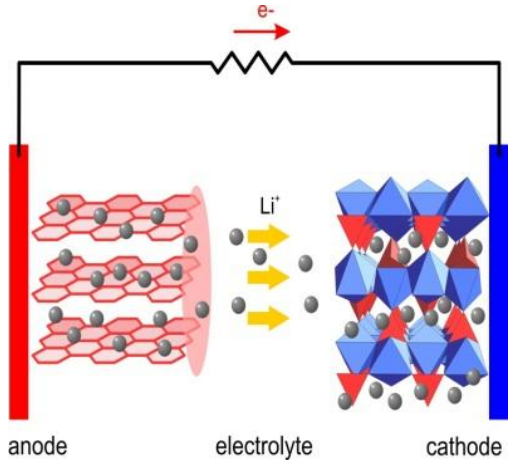

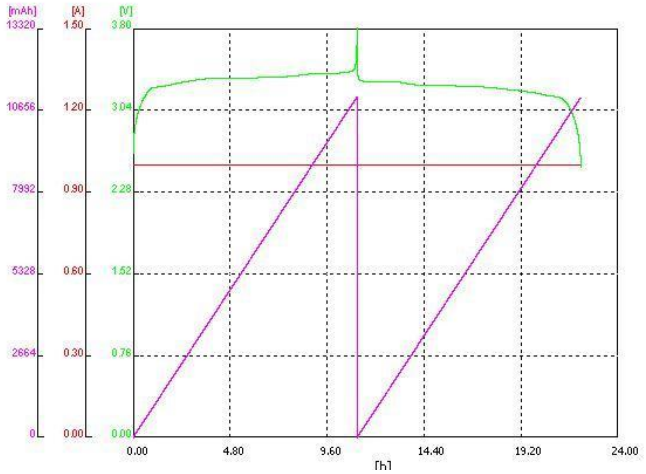

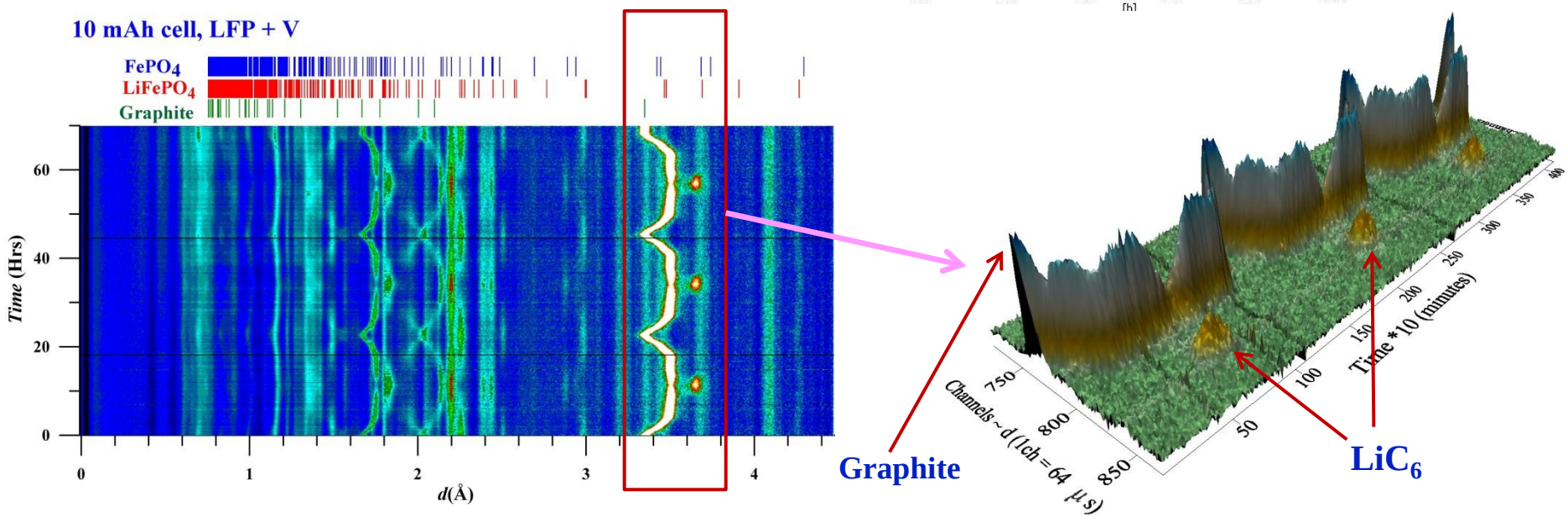

Evolution of neutron diffraction patterns of Li accumulator with $LiFePO_4$+*x*V working substance during three cycles of charging-discharging

I.A.Bobrikov et al., J. Power Sources (2014)

The pressure induced changes in magnetic structure of RCo_2

Exploring the nature of Itinerant Electron Metamagnetism phenomena in RCo_2

JINR - Babes-Bolyai University (Romania)

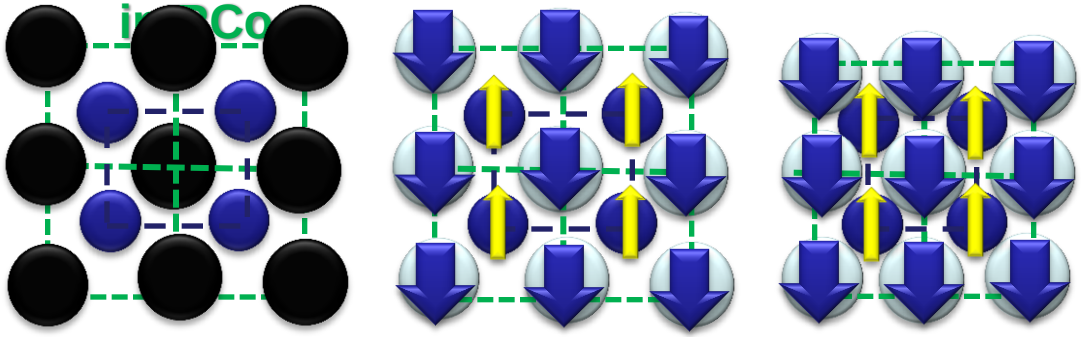

Non-magnetic R-ions

$M_R=0$

$M_{co}=0$

Magnetic R-ions

M_{Ho}~9.5 μ_B

M_{co} ~ 1 μ_B

Tuning the magnetic interaction by **pressure**

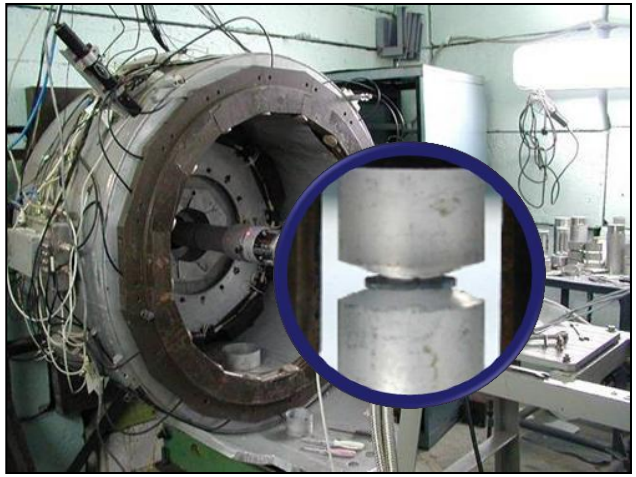

DN-12 neutron diffractometer

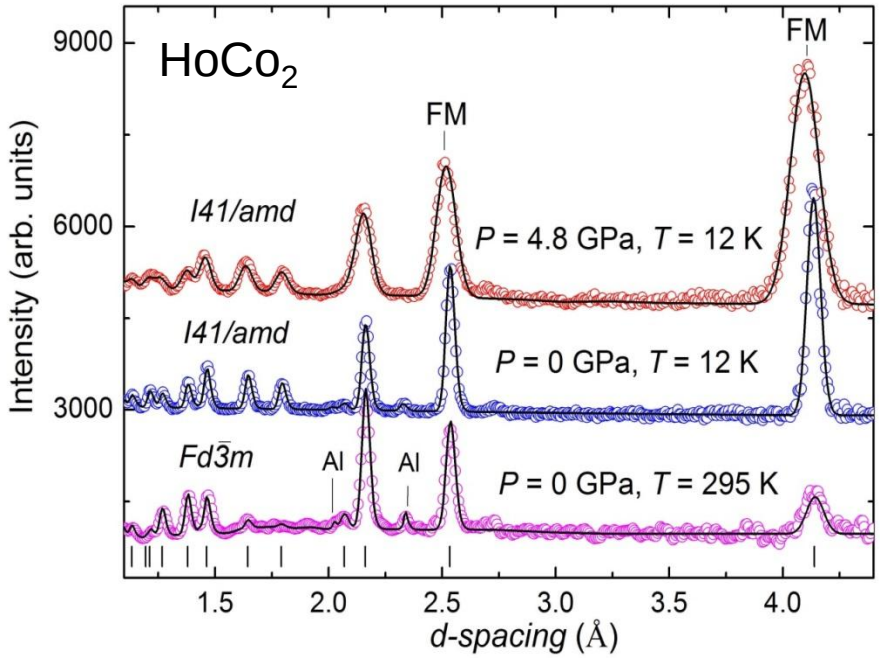

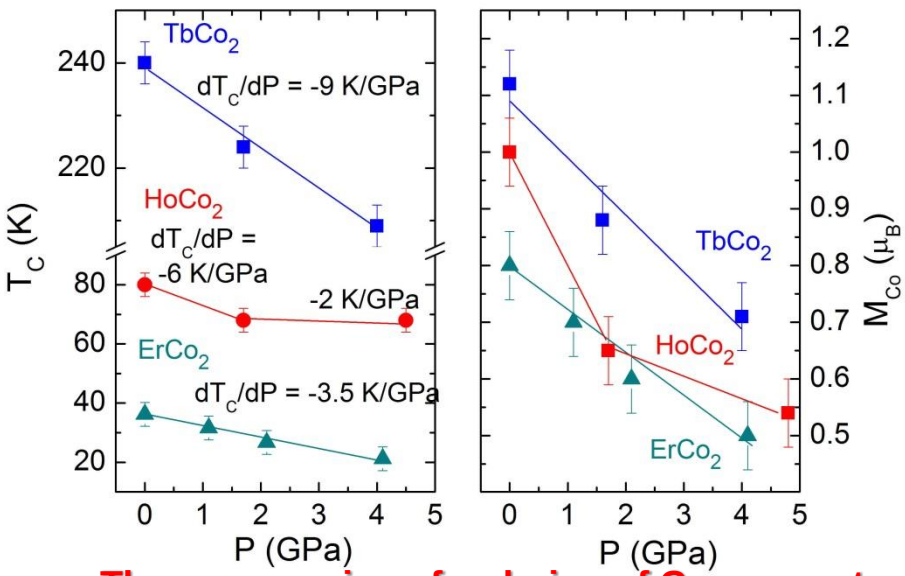

The suppression of ordering of Co moments

E.Burzo et al., J. Alloys and Compounds (2014)

Structural organization of nanodiamonds in liquid dispersions

Continuous spatial transition of carbon states in detonation diamonds liquid dispersions from crystalline diamond (sp^3-hybridization) inside particles to graphite-like state (sp^2-hybridization) on surface

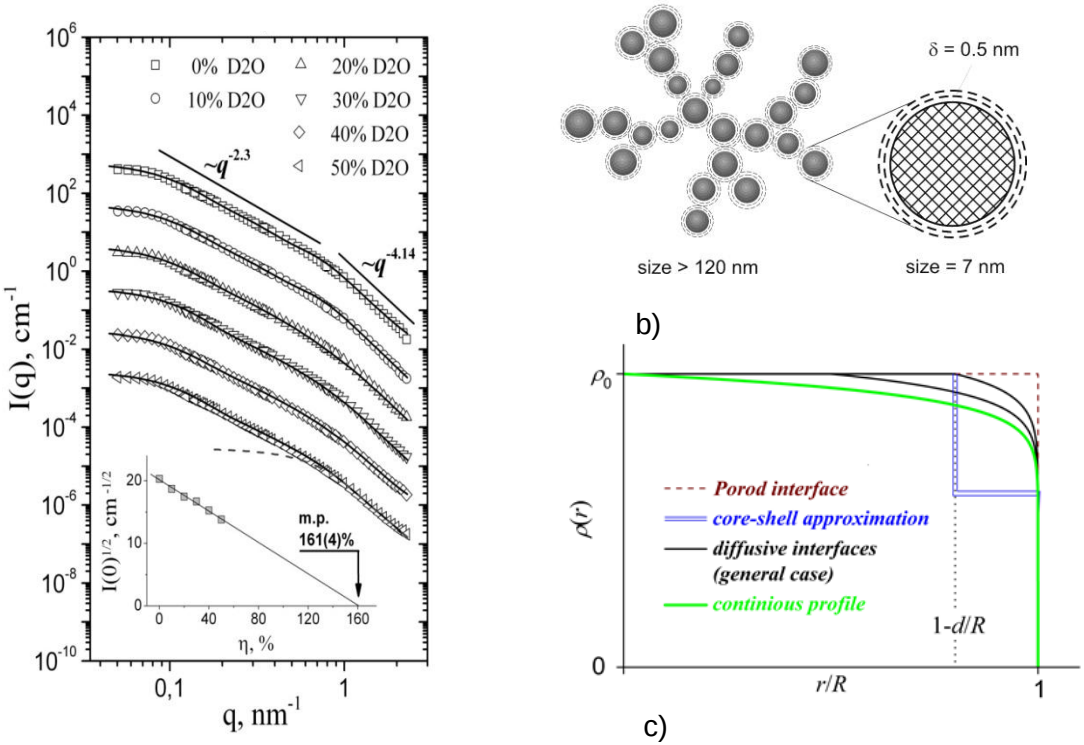

Experimental curves of small-angle neutron scattering from liquid dispersions of detonation nanodiamonds (DNA) measured with the contrast variation (a). A schematic view of a DNS cluster in liquid dispersions with an enlarged schematic representation of its basic structural unit - a particle composed of crystalline diamond and graphene shell (b). Various approximations to this shell are considered. A continuous diffusive profile (green solid line) gives the best fits to the experimental curves (c).

M.V.Avdeev et al., J. Phys. Condens. Matter (2013)

Small angle neutron scattering investigations of highly elastic magnetic elastomer samples

JINR - IFIN-HH (Romania)

SIEL elastomer with Fe microparticles and nanoparticles

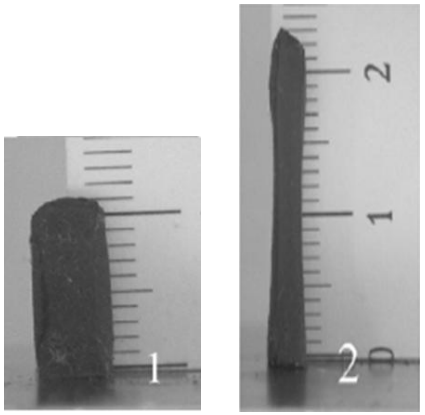

Shape memory effect:

1. H_0= 206 *kA* m^{-1}; non stretched
2. H_0= 206 *kA* m^{-1}; stretched by 80% and then unloaded retains its shape for hours.

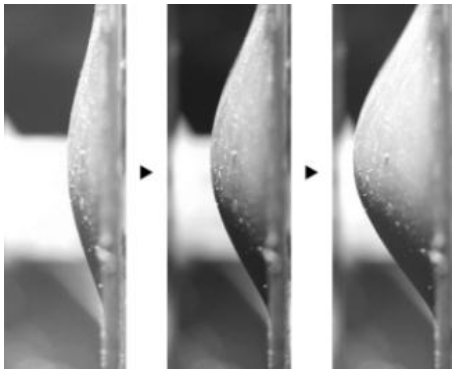

H_0=50 kA m^{-1} H_0=80 kA m^{-1} H_0=110 kA m^{-1}

Deformation of a membrane (D/h=10) in uniform transversal magnetic field H_0

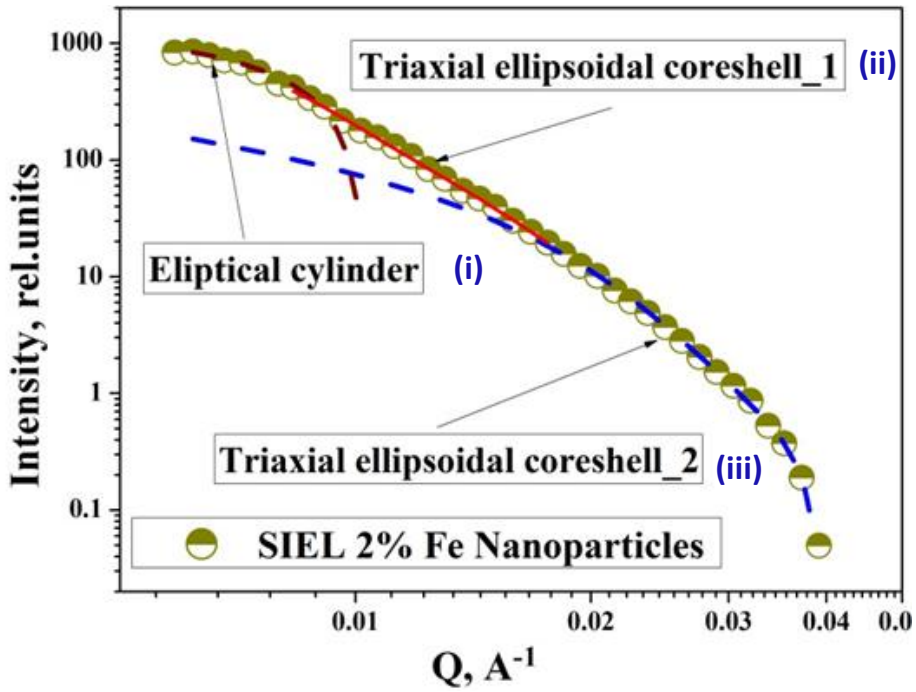

L~ 600 Å

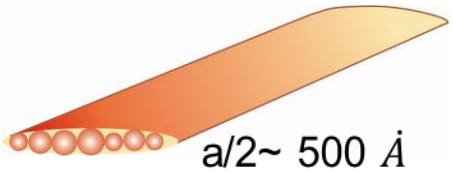

(i) Elliptical cylinder

a/2~ 500 Å

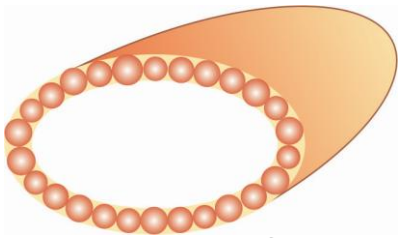

(ii) Triaxial ellipsoidal coreshell_1

a/2~ 250 Å

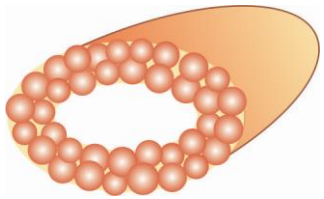

(iii) Triaxial ellipsoidal coreshell_2

M. Balasoiu, G. Stepanov, Yu. Raikher et al, 2014 (in preparation)

Unbinding transition of the lipid membranes at small concentrations of Ca^{2+} ions

JINR – MIPT (Russia)

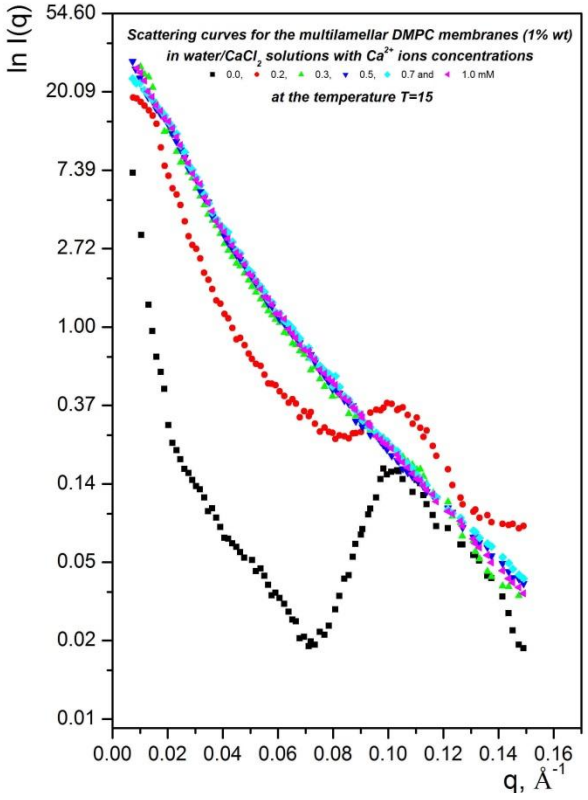

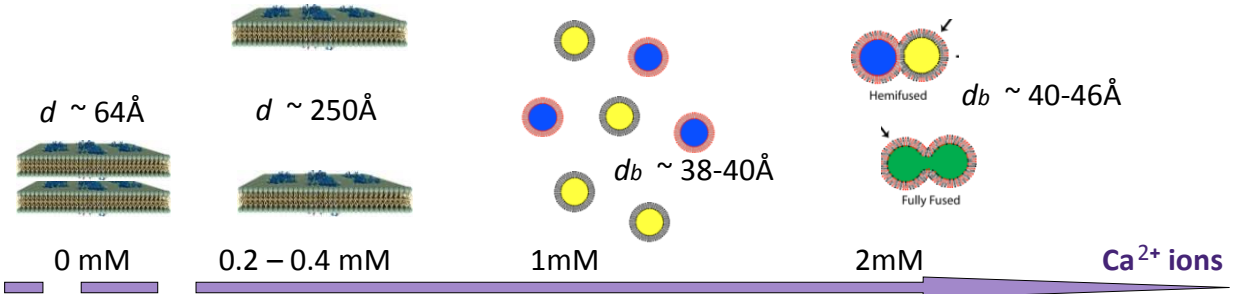

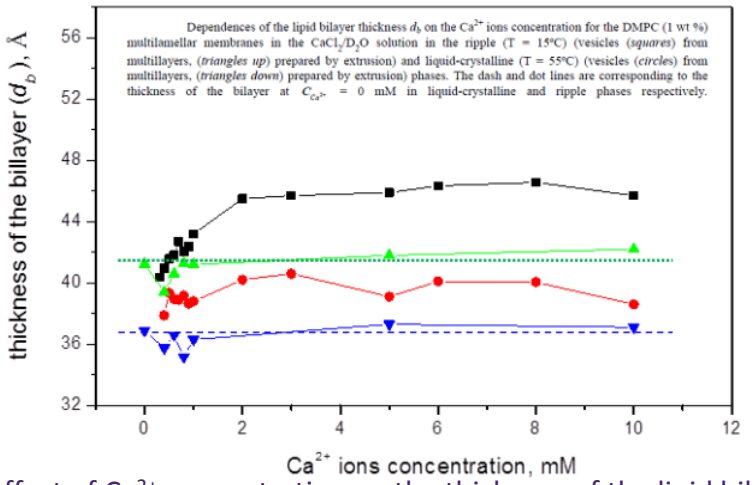

The studies of the effect of Ca^{2+} concentration on the thickness of the lipid bilayers possibly explain **why calcium**, causing a partial fusion of the single vesicles in the range of $0.3\text{mM} \leq C_{Ca^{2+}} \leq 2\text{mM}$, **is a necessary component in the final stages of the exocytosis.**

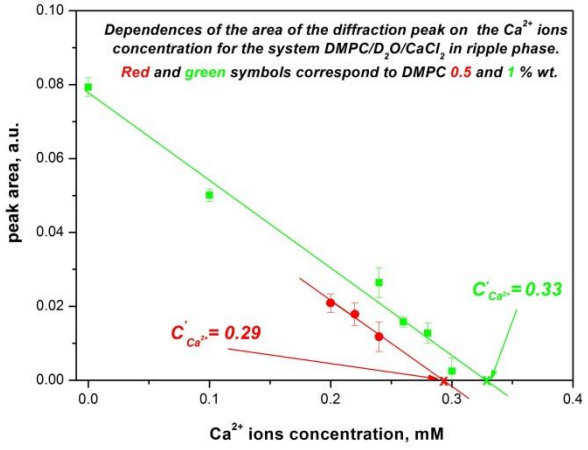

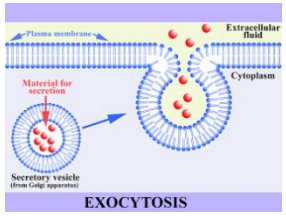

fusion of a cytoplasmic vesicle with the plasma membrane

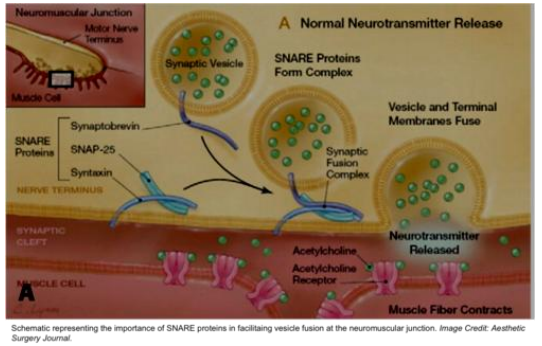

Schematic representing the importance of SNARE proteins in facilitating vesicle fusion at the neuromuscular junction. *Image Credit: Aesthetic Surgery Journal.*

Experimental and theoretical study of molecular dynamics and crystal structure of hexafluoroposphate (ESP-PF6) и tosylate (ESP-TOS) salts of alkylcoumarine derivatives – photoinitiator compounds

JINR - Jagiellonian University and University of Technology (Krakow, Poland)

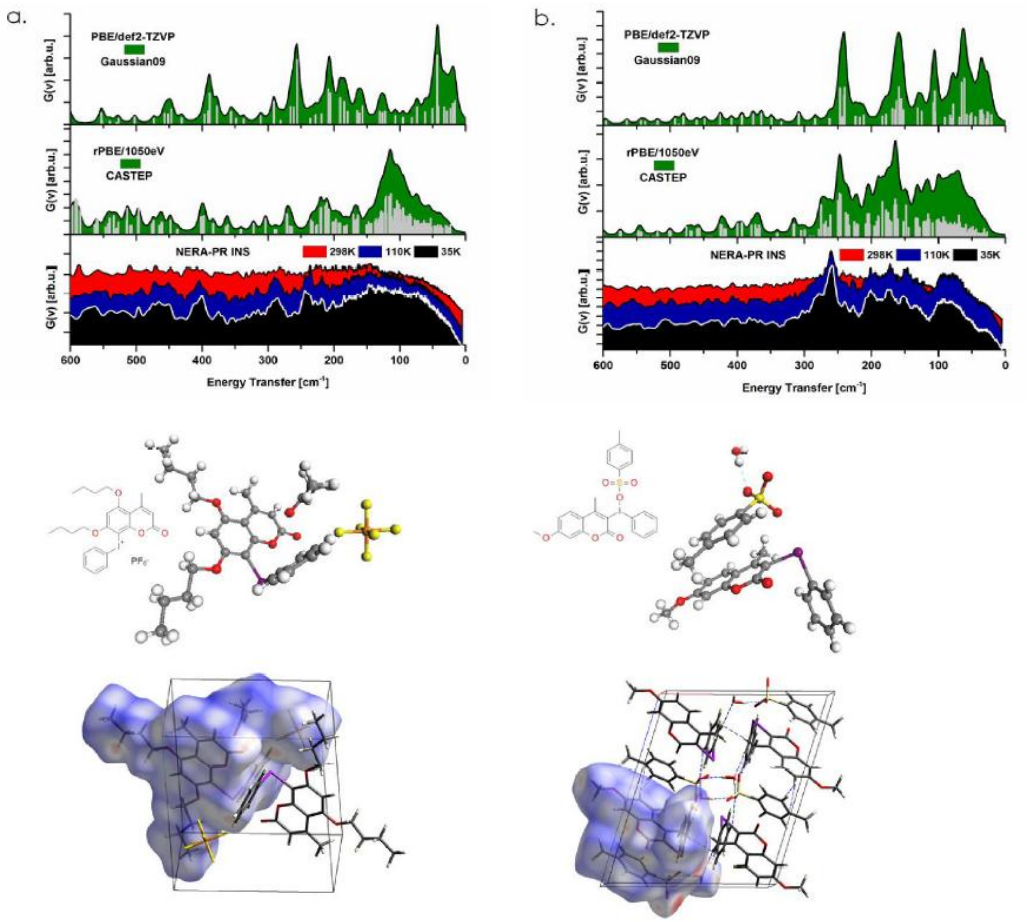

Inelastic neutron scattering spectra, results of theoretical modeling and crystal structure of ESP-PF6 (a) и ESP-TOS (b).

Residual stress in surveillance Charpy specimens, recovered by electron (EBW) and laser (LBW) beam welding

Collaboration: Institute of Electronics of BAS(Sofia, Bulgaria)
FLNP JINR (Dubna, Russia), NECSA Ltd. (Pretoria, South Africa)

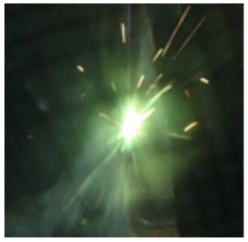

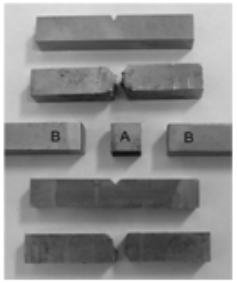

Electron beam welding

by Gizo Bokuchava (FLNP JINR) with colleagues: submitted to ***Nuclear Engineering and Design***

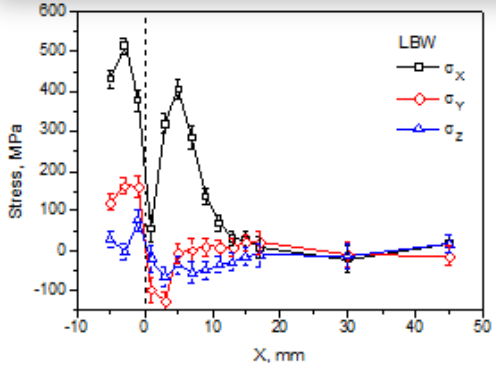

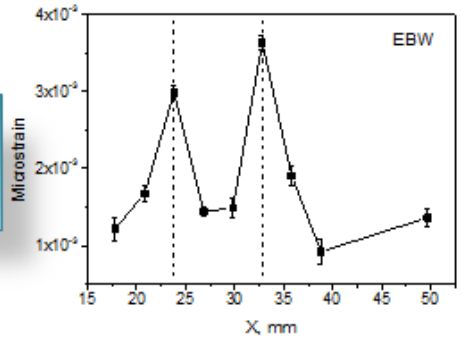

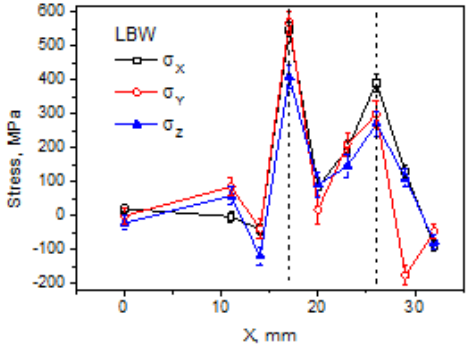

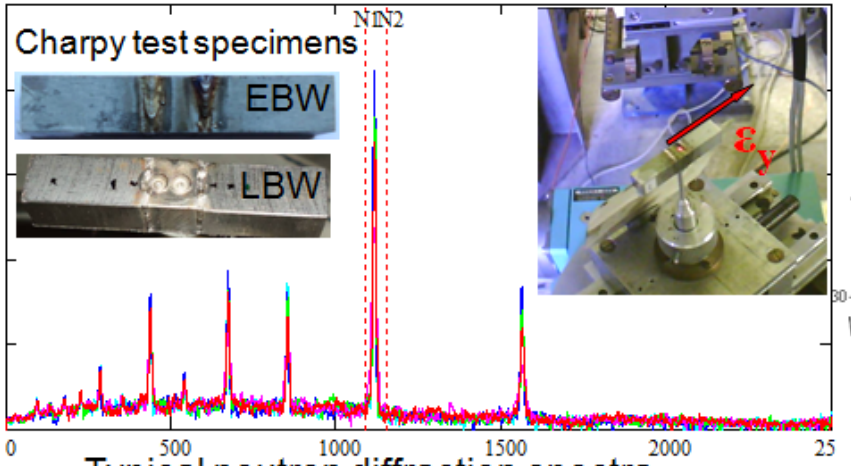

Typical neutron diffraction spectra

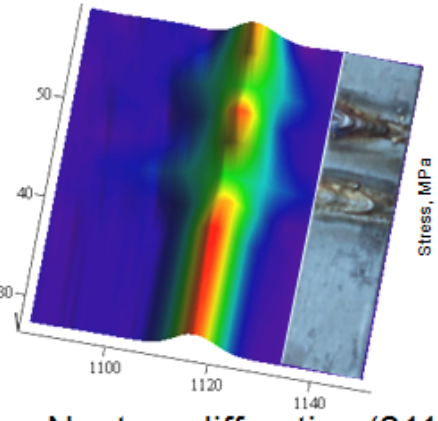

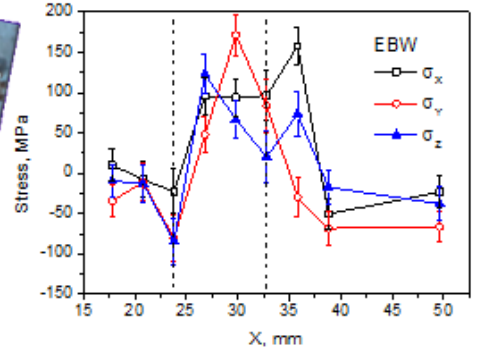

Neutron diffraction (211) reflection broadening at weld seam locations during x-scan

Neutron imaging of Seimchan meteorite

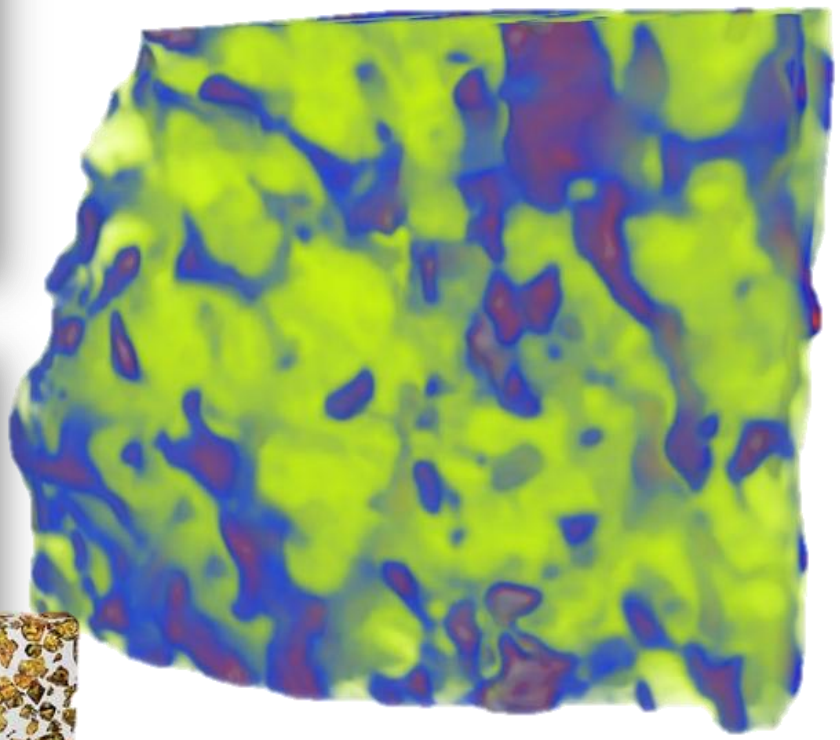

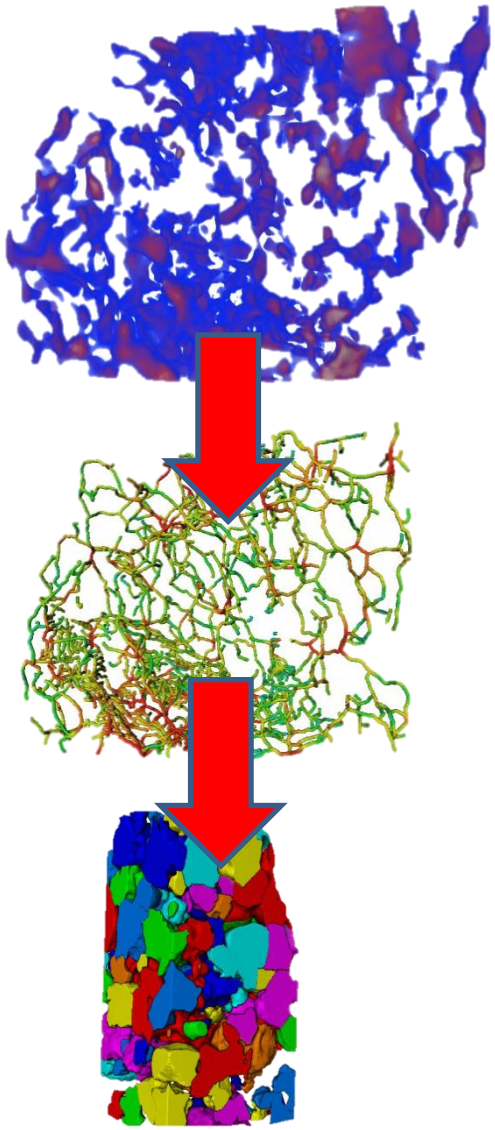

Neutron imaging of natural heritage objects

Paleontological Institute of RAS and
Paleontological Museum (Moscow)

Protosequoia cone (cretaceous period)

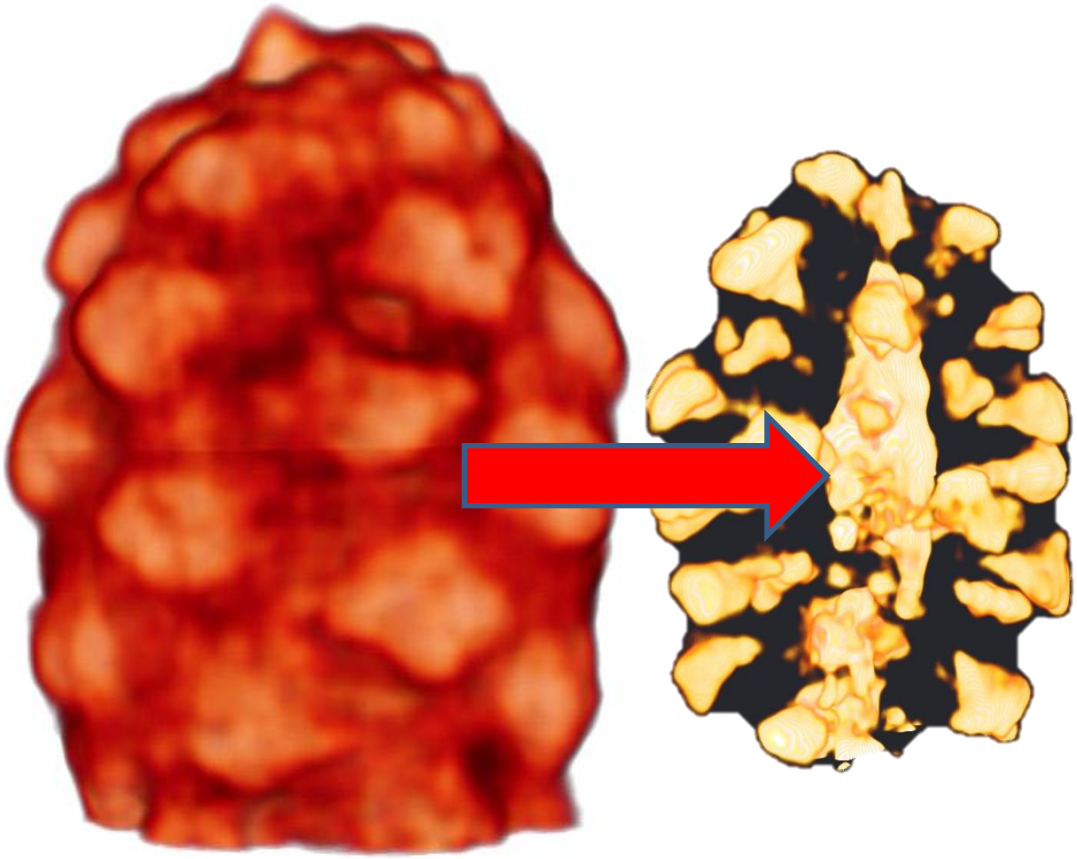


Thank You for Your Attention!